Not for Publication
Presented Before the Division of Gas and Fuel Chemistry
American Chemical Society
Atlantic City, New Jersey, Meeting, September 13-18, 1959

Physicochemical Properties of Green River Oil Shale, Particle Size and Particle-Size Distribution of the Inorganic Constituents

P. R. Tisot and W. I. R. Murphy

Laramie Petroleum Research Center
Bureau of Mines, U. S. Department of the Interior
Laramie, Wyoming

This paper presents information obtained regarding particle size and particle-size distribution of the inorganic constituents of Green River oil shale. Oil shale, a stratigraphic rock composed of a complex mixture of organic and inorganic constituents in variable proportions, is one of our major potential sources of liquid fuels. Pyrolysis is the basic principle common to the many experimental methods devised for converting the organic matter to liquid products. Many retorting systems have been developed, some to commercial or semicommercial scale (4,10,11). The similarity in percentage of organic matter converted to oil in such widely differing processes as a batch analytical method (13) and various large pilot plants operated at retorting temperatures of 850° to 950° F., indicates that the maximum conversion obtainable of organic matter to liquid products is of the order of 66 percent, regardless of the method of applying thermal energy. The other products formed are approximately 9 percent gas and 25 percent coke which remains on the shale residue. The published data further indicate that the crude oils produced are of poor quality (1,8,12). A definite explanation of these phenomena are not known. Probably they are a function of the molecular structure of the organic matter, the nature of the organic-inorganic association, the preferred reaction mechanism in a thermal system, or a combination of these factors.

As only 66 percent of the organic matter is converted to liquid products and the resulting oils are of poor quality, it would be highly desirable to develop processes that would improve both yield and quality of oil, thereby enhancing the economy of oil shale. Comprehensive understanding of the fundamental properties and structure of oil shale may improve existing methods or may disclose leads for devising new and better processes for converting the organic matter to liquid products. In the light of this, part of the research in oil shale is directed to gain a better insight into its physicochemical structure.

This is the first of a series of papers. Fundamental properties of oil shale currently under investigation are: Particle size and particle-size distribution of the primary inorganic particles; pore structure of the inorganic constituents; surface area of the raw oil shale and the inorganic constituents; pore size, pore-size distribution, and permeability of the inorganic matrix devoid of organic matter; and type of bonding between the organic and inorganic constituents. Information of this nature regarding oil shale is virtually nonexistent.

Experimental

Oil shales that differed widely in oil yield (75 and 28.6 gallons per ton) were selected for this investigation. Samples were taken at random from 1-foot-sections of beds EF and B, respectively, of the Selective mine, Rifle, Colo. (14). The 2 samples, approximately 200 pounds each, were crushed to pass a 2-mesh-per-inch screen.

Representative samples were taken and prepared as needed from each of the crushed samples.

Preliminary Considerations and Tests

Particulate materials usually respond favorably to particle-size measurements, but this is not the case with the primary inorganic particles that form part of the highly consolidated organic-inorganic system that exists in oil shale. The term "primary inorganic particles" is designated to mean the individual inorganic crystals. These crystals are either partly or entirely encased by organic matter and in many instances are bound together, in varying degrees, with inorganic cementing agents. The extent of the inorganic cementation is a function of the organic content. No practical or effective method is known whereby particle-size analyses of the primary inorganic particles can be made as they naturally occur in oil shale. It therefore became necessary to isolate the inorganic constituents. Removal of the organic matter by solvent action would have been ideal, as then the inorganic constituents recovered would have retained essentially their initial characteristics. However, no single solvent or combination of solvents was found that effectively separated the organic matter. Since solvent action did not accomplish the desired separation, the organic matter was removed by thermal treatment.

It was essential for comparative purposes that the organic matter be removed from the inorganic phase under a consistent set of conditions for all of the studies utilizing organic-free mineral constituents. In some studies the organic-free mineral constituents were prepared from many pieces of oil shale to form a single sample, whereas other studies required that organic-free mineral constituents be prepared from individual pieces of oil shale in the form of cores 1-1/2 inches long and 1/2 inch in diameter. The conditions selected for removing the organic matter, based on a series of preliminary tests, were those found that removed the organic matter from oil-shale cores with minimum physical and chemical changes to the mineral constituents.

Preparation of Organic-Free Mineral Constituents

Figure 1 presents a schematic diagram of the steps taken to prepare the organic-free mineral constituents. Two composites consisting of 200 to 300 pieces of oil shale ranging in size from 0.25 to 0.375 inch were selected from (1-B) to represent the 75-gallon-per-ton oil shale. The individual fragments were large enough so that any size reduction sustained by the primary inorganic particles exposed at the surfaces of the individual fragments during crushing of the oil shale were considered negligible. The composite samples were placed in separate porcelain dishes, arranged in the form of a bed 1-1/2 inches thick, covered, and placed in an electric muffle at room temperature. A thermocouple was placed in the center of one of the samples to record the bed temperature. The samples were heated to 250° F. over a period of one hour. The temperature of the oil-shale sample was raised in increments of 100° F. per hour to 650° F. It was maintained at 650° F. for six hours, then raised to 675° F. for an additional six hours and then to 700° F., until degradation of the organic matter appeared to be complete. This procedure was followed to permit the organic matter to escape from the individual pieces of oil shale with minimum structural breakdown of the inorganic matrix. Degradation of essentially all the organic matter appeared to occur between 650° and 700° F. At this phase of the thermal treatment the individual pieces were encrusted with carbonaceous material. The porcelain dishes were uncovered, and the temperature was maintained at 700° F. for four hours. During this period the carbonaceous material began to disappear slowly. The temperature was raised to 725° F. and maintained at this point for four hours. Any carbonaceous material remaining was removed at 750° F. Chemical analyses indicated that the shale residue obtained from this treatment contained less than 0.1 weight-percent of the initial organic carbon.

Two composite samples of organic-free mineral constituents from 28.6-gallon-per-ton

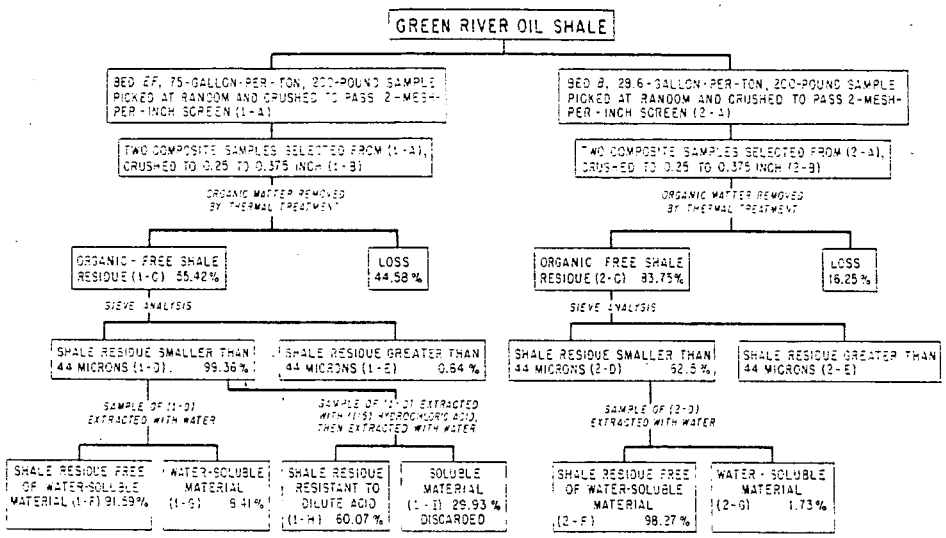

FIGURE 1.-SCHEMATIC DIAGRAM FOR PREPARING ORGANIC-FREE SHALE RESIDUE FOR PARTICLE-SIZE MEASUREMENTS

oil shale (2-C) were prepared in the same manner as described above. Oil shale of this degree of richness was selected, as it occurs at several different levels in the Selective mine. The inorganic mineral constituents recovered from the 75- and 28.6-gallon-per-ton oil shales represented 55.42 and 83.75 weight-percent of the initial oil shale, respectively.

Mineral Constituents

The major inorganic constituents in the oil shales studied were quartz, feldspars, dolomite, and calcite, which compose approximately 95 weight-percent of the total mineral matter. The minor constituents include illite clay minerals, pyrite, and analcite. The constituents most sensitive to thermal treatment are the illite clay minerals, pyrite, and the carbonates. Grim (2) has shown by differential thermal curves that illite does not undergo formation of new phases at 750° F., or below. According to Jukkola et al., (5) the dolomite and calcite in oil shale do not decompose below 1000° F. Samples of organic-free shale residue maintained at 750° F. for eight hours had an average loss in weight of 0.15 weight-percent indicating that the shale residue did not undergo any appreciable loss in weight on prolonged heating.

Chemical Changes During Thermal Treatment

As a result of chemical changes that occurred during removal of the organic matter, the shale residue (1-C) contained 5.07 weight-percent calcium sulfate and 4.51 weight-percent ferric oxide. Formation of these compounds introduced particles foreign to the original inorganic constituents, as calcium sulfate and ferric oxide have been identified in only trace amounts in the minable bed. The ferric oxide most likely resulted from oxidation of the iron pyrite, and the calcium sulfate probably was formed by interaction between calcite and either organic or inorganic sulfur or a combination of both. Apparently the calcite was attacked instead of the dolomite in the formation of calcium sulfate, as no magnesium sulfate or free magnesium carbonate was detected in the shale residue. The calcium sulfate could be removed by prolonged continuous extraction with water. Because of density difference between the ferric oxide and the remainder of the shale residue, the conglomerated ferric oxide could probably be removed by gravity separation, using an appropriate liquid medium. However, effective separation by this method was not accomplished. Failure to separate the ferric oxide was attributed to physical forces interacting between the fine particles and liquid medium. Therefore the ferric oxide was included as part of the shale residue.

Particle-Size Measurements, Sieve Analysis

Particle-size measurements of the larger particles in the rich shale residue were determined by passing each of the two composite samples (1-C) over 30-, 60-, 80-, 100-, 200-, 300-, and 325-mesh sieves and weighing the primary inorganic particles retained on each sieve. Any shale residue that did not readily pass successive sieves was moved over the screen surfaces by applying pressure with a small brush. This method reduced conglomerated masses but was not severe enough to fracture primary particles. Hence, any new particles formed in reducing the conglomerates by this method were essentially fragments of cementing agents or possibly of some of the illite clay minerals. The combined weight of the primary particles retained on the sieves, above 600 and down to 44 microns in diameter, amounted to 0.64 weight-percent of the shale residue (1-C).

Particle-Size Measurements in the Subsieve Range

Microscopic examinations of the shale residue in the subsieve range (1-D) revealed that it still contained conglomerated masses. Reduction of these masses, except for some of the ferric oxide, was best attained by subjecting the shale residue suspended in a liquid medium to ultrasonic vibrations. The apparatus used to produce the

ultrasonic vibrations was a Glennite Model U-621 ultrasonic unit rated at 44 kilocycles per second with a power output to the transducers of 100 watts. Primary particles of calcite and dolomite recovered on the 80- and 100-mesh sieves were exposed to ultrasonic vibrations without significant deleterious effects. From these observations it was concluded that the ultrasonic vibrations induced no appreciable shatter of the primary particles.

Each composite sample of shale residue in the subsieve range (1-D) was divided into three portions, as it was desired to obtain particle-size information of the initial shale residue (1-D), the shale residue free of water-soluble material (1-F), and that portion of the shale residue resistant to dilute hydrochloric acid (1-H). The water-soluble-free and acid-resistant residues represented 91.59 and 60.07 weight-percent of the initial shale residue (1-C). The respective specific gravities of the three residues were 2.7443, 2.7354, and 2.6892. The continuous water extraction removed 3.34 weight-percent of material other than calcium sulfate from the initial shale residue (1-D).

Many different methods and apparatus, each with its merits and limitations, are used for making particle-size measurements of materials in the subsieve range (6,15). The method selected for this work was the increment method of sedimentation, considered to be one of the most accurate methods; the apparatus was an Andreasen sedimentation vessel. One limitation of this method is that particles with diameters smaller than 0.5 micron cannot be measured owing to Brownian movement, which prevents free fall. Two important requirements for accurate particle-size measurements are a high degree of dispersion of individual particles and subsequent prevention of flocculation during the prolonged test period. These requirements were best attained when a suspension medium was used that consisted of distilled water containing 2 grams per liter of Daxad No. 23 as the dispersing agent (7). Periodic examination of the suspension and the formation on standing of a rigid sediment of minimum volume indicated that the two requirements were attained to a high degree.

Duplicate determinations were made on each of samples (1-D), (1-F), and (1-H). A weighed sample, sufficient to give an approximate volume concentration of 1 percent of the volume of the sedimentation vessel, was mixed with 200 ml. of suspension medium; and the suspension was subjected, with constant stirring, to ultrasonic vibrations for 30 minutes. The mixture was transferred to the sedimentation vessel, diluted to the reference mark with suspension medium, and thoroughly mixed before it was placed in a constant-temperature bath (70° F.) to minimize the effects of convection currents. The suspension medium used to analyze (1-D) was saturated at 70° F. with calcium sulfate to prevent any calcium sulfate in the shale residue from going into solution. After temperature equilibrium was attained, the vessel was removed, thoroughly shaken for several minutes, employing a tumbling motion, returned to the bath, and the first 10-ml. fraction immediately withdrawn and transferred to a tared beaker. Subsequent fractions were withdrawn and transferred to tared beakers at increasing time intervals, arbitrarily selected over a cumulative period of about 100 hours per analysis. Each fraction except the first was withdrawn at uniform rate, approximately 20 seconds per fraction, to minimize disturbance of the suspension. The number of fractions collected totaled 20 to 22. After evaporation of the liquid and drying at 220° F., each fraction was weighed and the correction applied for the dispersing agent. The corrected weight of the first fraction represented the initial concentration of shale residue in the suspension. The weight-percent of each subsequent fraction was calculated from the initial concentration, and its corresponding particle size was determined by Stokes' law, expressed as follows: (9)

$$r = \sqrt{\frac{9\,h\,n}{2(d_1-d_2)\,g\,t}},$$

where r is the radius of spherical particle (cm.); n, the viscosity of suspending medium (poises); h, distance (cm.) between liquid surface and pipette tip when sample is withdrawn; d_1, specific gravity of the particle; d_2, specific gravity of suspending medium; g, gravitational constant; and t, time in seconds. Stokes' law is based on the premise that particles are spherical and smooth and that the concentration of the suspension is dilute enough to permit free fall. Photomicrographs (Figures 2, 3, 4, and 5) revealed that the primary particles were essentially nonspherical. However, Lamar (7) states that irregular particles within the subsieve range have been shown to behave much like spheres. Hence, the results obtained by the sedimentation method should be valid.

The shale residue (2-C) from the 28.6-gallon-per-ton oil shale was subjected to a sieve analysis in the same manner described for the shale residue from the rich oil shale. The degree of cementation between individual primary particles was fairly extensive. As a result of this, only 62.5 weight-percent of the shale residue was reduced to within the subsieve range. Ultrasonic treatment did not effectively reduce the conglomerated masses retained on the sieves. To further reduce them would have required some form of crushing. Because of the high degree of cementation and low percentage (1.73) of water-soluble material (2-C), only the initial material in the subsieve range (2-D) was analyzed for particle size.

Interpretation of Results

Mathematical analysis of the direct analytical data from the sedimentation runs indicated that these data could best be expressed by converting them to a form that permitted graphic presentation, that is, cumulative weight-percent oversize as a function of the logarithm of equivalent spherical diameters. Figure 6 presents the cumulative size-distribution curve for the initial oil-shale residue (1-C). The linear plot represents the sieve analysis. If the primary particles had been spheres, the S-shaped curve would not show particles with diameters greater than 44 microns, as they would have been retained on the 325-mesh sieve. Overlapping of the two curves is attributed partly or entirely to the principle that sieves classify particles according to the least cross-sectional area. The material that remained in suspension after completion of the sedimentation run (7.20 weight-percent, with equivalent spherical diameters of less than 0.5 micron) was essentially calcium sulfate and illite clay minerals, as determined by X-ray diffraction. The total quantity of shale residue accounted for was 99.5 weight-percent of the shale residue analyzed.

Figure 7 presents the cumulative particle-size distribution curve of shale residue free of water-soluble material (1-F). The S-shaped curve represents the average particle size based on the analytical data from two composite samples. The degree of conformity between the two samples, as exhibited by the plotted points, was such that only one curve could be conveniently presented. The linear plot represents the sieve analysis. The total quantity of shale residue accounted for represented 98.8 weight-percent of the shale residue analyzed, of which 3.2 weight-percent remained in suspension. The material that remained in suspension was essentially illite clay minerals.

The cumulative particle-size distribution curve for the shale residue treated with dilute hydrochloric acid (1-H) is shown in Figure 8. The major constituents in the acid-resistant residue were quartz and feldspars. The S-shaped curve represents the average of two sets of experimental data taken from two composite samples of shale residue. The plotted points show the actual values calculated from the analytical data. The quantity of shale residue with equivalent spherical diameters less than 0.5 micron that remained in the suspension medium at the end of the run was 2.6 weight-percent. The total quantity of shale residue accounted for was 98.5 weight-percent of the shale residue charged to the sedimentation vessel.

Figure 9 presents the cumulative particle-size-distribution curve for the primary

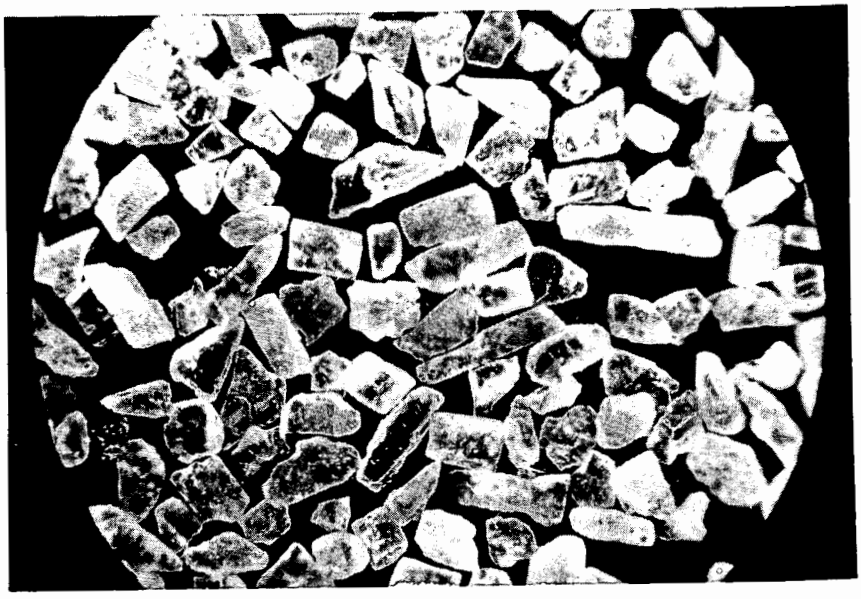

Figure 2. Photomicrograph of primary inorganic particles illustrating shape and roundness. Equivalent spherical diameter range, 175 to 250 microns. Magnification 30X.

Figure 3. Photomicrograph of primary inorganic particles shown above. Magnification 100X.

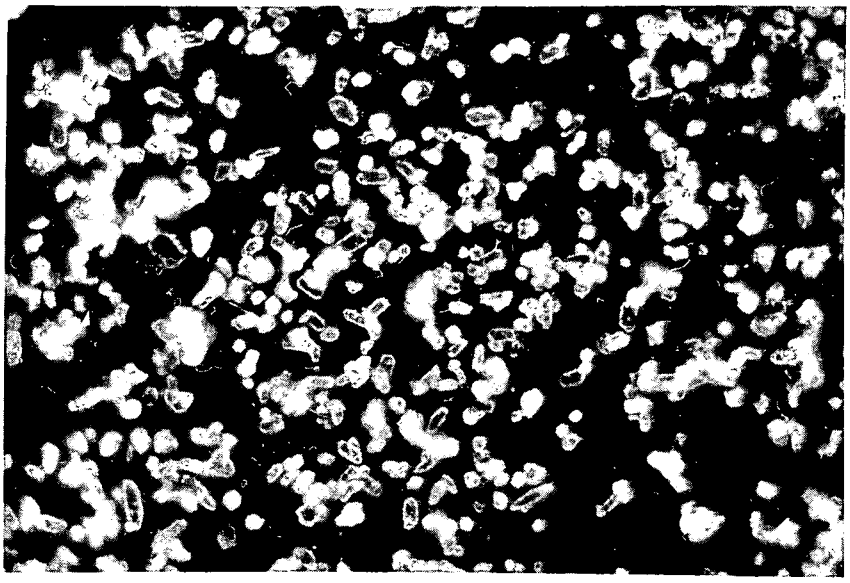

Figure 4. Photomicrograph of primary inorganic particles. Equivalent spherical diameter range, 5 to 15 microns. Magnification 210X.

Figure 5. Photomicrograph of primary inorganic particles, essentially quartz and feldspars. Equivalent spherical diameter range, 15 to 30 microns. Magnification 210X.

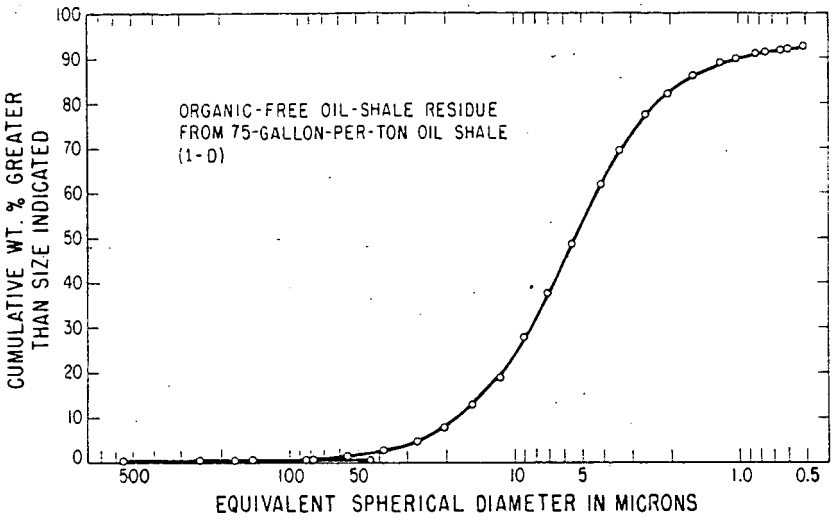

FIGURE 6.-CUMULATIVE PARTICLE-SIZE DISTRIBUTION CURVE OF THE PRIMARY INORGANIC PARTICLES IN RICH OIL SHALE

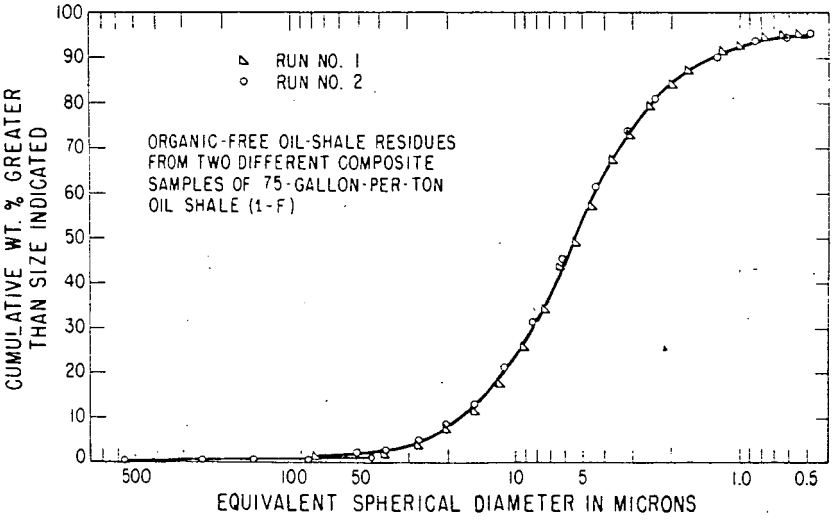

FIGURE 7.-CUMULATIVE PARTICLE-SIZE DISTRIBUTION CURVE OF PRIMARY INORGANIC PARTICLES FREE OF WATER-SOLUBLE MATERIAL

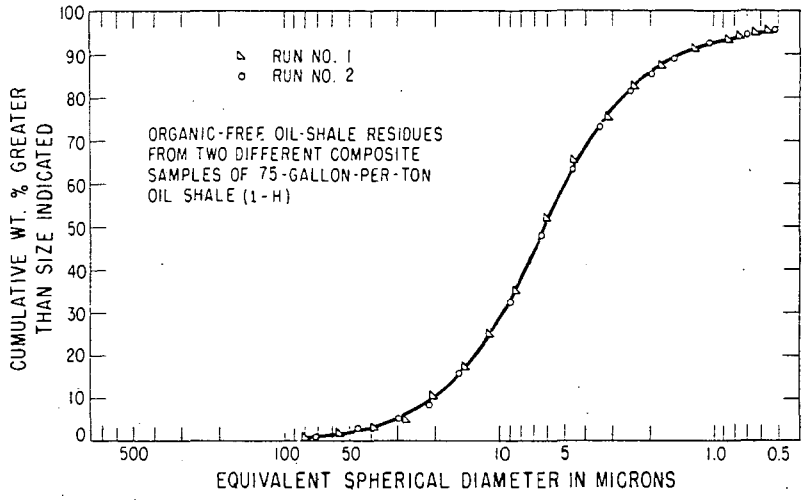

FIGURE 8.-CUMULATIVE PARTICLE-SIZE DISTRIBUTION CURVE OF PRIMARY INORGANIC PARTICLES FREE OF WATER-SOLUBLE AND DILUTE MINERAL ACID-SOLUBLE MATERIALS

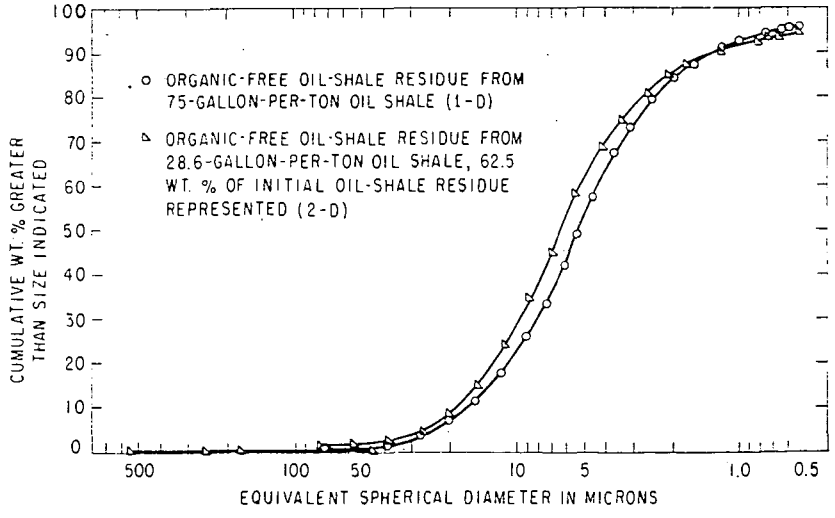

FIGURE 9.-CUMULATIVE PARTICLE-SIZE DISTRIBUTION CURVES OF PRIMARY INORGANIC PARTICLES IN 75-AND 28.6-GALLON-PER-TON OIL SHALE

inorganic particles (2-D), 28.6-gallon-per-ton oil shale, that passed through the 325-mesh sieve. The plot of Figure 6 is included in Figure 9 for the purpose of comparing particle size and particle-size distribution of primary inorganic particles in oil shale taken at two different levels within the oil-shale formation. The oil shales from these two levels differed widely in organic content. It is noted that both size and distribution of the primary particles within the two levels exhibit a high degree of similarity. Microscopic examination of the portion of the shale residue that did not reduce to primary particles (2-E) during the screen analysis indicated that the sizes of the primary particles constituting the conglomerated masses were of the order of those that passed the 325-mesh sieve.

The direct results of all the sedimentation analyses in the form of cumulative weight-percent oversize as a function of equivalent spherical diameters in microns plotted as S-shaped curves. The plots indicate that distribution of sizes of the primary inorganic particles in Green River oil shale tends to follow a log-normal distribution. Good agreement to log-normal distribution was noted between equivalent spherical diameters ranging from approximately 1.7 to 35 microns when these data were plotted on logarithmic probability paper. Departure from log-normal distribution was noted above and below these diameters. Cumulative frequency curves that are log-normal plot as linear lines on logarithmic probability paper. Information available from the cumulative frequency curves are, particle-size range of the primary inorganic particles, weight-percent of shale residue above or below a given diameter, or weight-percent of shale residue within any two size ranges except for the shale residue smaller than 0.5 micron. Two parameters that normally define distribution curves of this type (geometric mean size and standard geometric deviation) may be calculated from the S-shaped curves by reading appropriate intercepts. The geometric mean size is the value in microns corresponding to 50-weight-percent oversize, and the standard geometric deviation is the ratio of sizes corresponding either to 84.13 and 50.00 or 50.00 and 15.87 weight-percent oversize (3). The geometric mean sizes of the primary inorganic particles determined from the distribution curves of shale residues represented by (1-D), (1-F), (1-H), and (2-D) were 5.3, 5.4, 6.2 and 6.4 microns, respectively. The values of the standard geometric deviations for the above curves, as calculated from the ratio of sizes corresponding to 84.13 and 50.00 percent oversize, were 0.3, 0.4, 0.4, and 0.3, respectively. Calculated from the ratio of sizes corresponding to 50.00 and 15.87, the values obtained for the standard geometric deviation were 0.4.

Geometric Form of Primary Inorganic Particles

Information concerning two fundamental properties of the primary inorganic particles -- shape and roundness -- is best conveyed with photomicrographs. Figure 2 illustrates primary inorganic particles retained on a minus 60-plus 80-mesh sieve. The particles are predominantly rhombic. Increased magnification of a number of these particles brings out the third dimension and some of their surface characteristics, as noted in Figure 3. Figure 4 illustrates primary particles with equivalent spherical diameters ranging from 5 to 15 microns. The geometric configuration of the primary particles, with equivalent spherical diameters smaller than 5 microns, could not be brought out clearly with photomicrographs. However, microscopic examination of these particles revealed that their geometric form resembled that shown in Figure 4. Figure 5 illustrates the primary particles that were resistant to dilute hydrochloric acid. The equivalent spherical diameter of these particles, essentially quartz and feldspars, ranged from 15 to 30 microns. X-ray analyses indicated that the sharp-pointed particles were quartz.

Summary

The results of this investigation provide better understanding of the particle

size, particle-size distribution, and geometric form of the primary inorganic particles present in Green River oil shale. Because particle-size studies could not be made in the presence of the organic matter, it was removed by thermal treatment in a manner that minimized chemical and physical changes to the mineral constituents. By virtue of its high organic content, oil shale that assayed 75 gallons per ton yielded a friable residue amenable to this type of work. The portion of shale residue from the 28.6-gallon-per-ton oil shale that reduced to primary inorganic particles without crushing -- 62.5 weight-percent -- was used for particle-size studies.

The primary inorganic particles were essentially nonspherical, and their predominate geometric form appeared to be rhombic. More than 99 weight-percent of the primary inorganic particles analyzed had equivalent spherical diameters less than 44 microns. The distribution of sizes tend to follow a log-normal distribution between equivalent spherical diameters ranging from 1.7 to 35 microns. Departure from log-normal occurred below and above these values. The geometric mean size and standard geometric deviation of the primary inorganic particles free of water-soluble material in the 75-gallon-per-ton oil shale were 5.4 microns and 0.4, respectively. The corresponding values for that portion of the 28.6-gallon-per-ton oil shale residue analyzed were 6.4 microns and 0.3. The range of sizes and type of distribution of the primary inorganic particles of oil shales that differed widely in organic content and represented two different levels within the Green River formation appeared to be quite similar.

Acknowledgment

This project was conducted at the Laramie Petroleum Research Center, Laramie, Wyo. under the general direction of H. M. Thorne. The authors gratefully acknowledge the help of H. N. Smith, W. A. Robb, and J. A. Lanun for x-ray analyses and some of the analytical work. This work was done under a cooperative agreement between the University of Wyoming and the U. S. Bureau of Mines, Department of the Interior.

Literature Cited

(1) Cameron, J. B., Guthrie, B., Chem. Eng. Prog. 50 No. 7, 336 (1954).
(2) Grim, R. E., "Clay Mineralogy," McGraw Hill, New York, 238 (1953).
(3) Hatch, T., Choate, S. P., Jour, Fran. Inst. 207, 373 (1929).
(4) Hull, Q. W., Guthrie, B., Sipprelle, E. M., Liquid Fuels from Oil Shale, A Staff-Industry Collaborative Report, Ind. Eng. Chem. Vol. 43, 2 (1951).
(5) Jukkola, E. E., Denilauler, A. J., Jensen, H. B., Barnet, W. I., Murphy, W. I. R., Ind. Eng. Chem., 45, 2714 (1953).
(6) Lamarr, R. S., Amer. Ceram. Soc. Bull. 31, 283 (1952).
(7) Ibid, 285.
(8) Langford, J. D., Ellis, C. F., Ind. Eng. Chem. 43, 28 (1957).
(9) Loomis, G. A., Jour. Amer. Ceram. Soc. 21, No. 9, 398 (1938).
(10) McKee, R. H., "Shale Oil", The Chemical Catalog Co. Inc., New York, 150 (1925).
(11) "Oil Shale and Cannel Coal", The Institute of Petroleum, Manson House, 26 Portland Place, London, W. 1, 345 (1951).
(12) Ibid, 502.
(13) Stanfield, K. E., Frost, I. C., McAuley, W. S., Smith, H. N., Bur. of Mines Rept. Invest. 4825, 18 (November 1951).
(14) Ibid, 4.
(15) Symposium on New Methods of Particle-Size Determination in the Subsieve Range, A. S. T. M. Spec. Tech. Bull. No. 51 (Mar. 4, 1951).

Not for Publication
Presented Before the Division of Gas and Fuel Chemistry
American Chemical Society
Atlantic City, New Jersey, Meeting, September 13-18,1959

The Geometric Area Shape Factors of Coals Ground in a Standard Hardgrove Mill

L.G. Austin, R.P. Gardner, and P.L. Walker, Jr.
Fuel Technology Department, The Pennsylvania State University
University Park, Pennsylvania

INTRODUCTION

The relation of energy input on grinding to the production of fresh broken surface has received much study (1); and, consequently, comparative increases in surface areas of ground particles have been measured by a variety of methods. However, the absolute external or geometric surface area of coal particles, and the corresponding shape factor, have significance in other processes than grinding. For instance, in processes where coal is chemically reacted at high rates, the rate of reaction is partially controlled by the geometric area (2). The area of any sample of coal of which the density and sieve size distribution are known can be readily calculated from a knowledge of a shape factor k defined by

$$(\text{geometric surface area})\ \mu = k\ (\text{volume}) \qquad (1)$$

where μ is a sieve size. Aris (3) has shown that the ratio of volume to geometric area, that is μ/k, is a characteristic dimension for use in studies of the reaction of solids in beds. Hawksley (4) considers that the drag diameter, which is approximately equal to the diameter of the sphere having the same surface area as the particle, is the most fundamental dimension for use in hydrodynamic problems involving particles. The drag diameter is related to the sieve size by

$$d = \frac{6\mu}{k} \qquad (2)$$

The above remarks indicate that a knowledge of the values of k for coals is likely to be of interest in many industrial processes. Examples of such processes where the shape factor is of actual or potential importance are:

(a) the combustion of pulverized coal in central power stations,
(b) the gasification of pulverized coal,
(c) the production of low temperature coke and coal chemicals in fluidized bed processes,
(d) the firing of open cycle turbines with pulverized coal,
(e) the hydrogenation and chemical processing of coal suspensions, and
(f) the transport of coal in fluid suspensions.

REVIEW OF PREVIOUS WORK

As is well known, coal has a large internal surface area due to a very fine micropore system within the particle (5). Many methods of measurement of surface area determine this internal area in addition to the exterior

surface and, therefore, are not suitable for the measurement of shape factors. The fluid permeability technique, utilizing a modified Kozeny equation, does not in general measure internal surface area (6). This is so because the internal pore system of coal has a negligible permeability compared to the flow between coal particles in a packed bed. Romer (7) used an air permeability method to measure the geometric surface area of ground coal fractions. He did not, however, make available enough information to enable shape factors to be calculated. Skinner (8) pointed out that the hydrodynamic area as measured by permeability methods is of primary importance in the combustion of pulverized fuels and recommended that it should be used to measure shape factors instead of assuming a constant shape factor with size.

APPARATUS AND EXPERIMENTAL TECHNIQUE

Grinding of Coal--The coal under test was ground in a standard Hardgrove test machine according to the A.S.T.M. standard method (9). The ground product was carefully sieved into fractions and the fractions weighed. These fractions were then used for the density and surface area measurements described below.

Density of Coal Fractions--To measure the surface area by the permeability method, it was necessary to know the apparent density of the coal particles tested. Apparent densities were determined, at first, by water displacement in a specific gravity bottle. The coal powder was weighed, vigorously stirred with water to thoroughly wet and release entrapped air, and the density determined. The operation could be carried out in a few minutes and it was thought that in this time the water would not penetrate the internal porosity of the coal to any marked extent. This method gave reproducible results for the larger mesh fractions, but it was found difficult to wet and de-aerate the fine mesh fractions (-200 mesh). Consequently, mercury densities were determined using a mercury porosimeter (10). The pressure of mercury was increased until the rate of entry of mercury dropped suddenly and further pressure caused only a small further penetration. The sudden change-point was taken as equivalent to the geometric density, and the slow additional penetration as the filling of the internal pore system of the particles.

Measurement of Surface Area of Coal Fractions--The surface areas of the coal fractions were determined using the liquid permeability apparatus described by Lakhanpal, Anand and Puri (11) and shown in Figure 1. A coal sample was weighed and packed into tube A, being supported by a thin pad of glass wool over the constriction in the tube. The time taken for a given volume of water to flow through the bed under the mercury head was noted, as were the initial and final mercury heads, suitably corrected for the water pressure head on the right hand column of mercury, Δl. From the weight and density of the coal sample, the diameters of tubes A and C (determined by mercury calibration), the length of the bed, and the viscosity of water at the temperature of the experiment, the surface area of the coal in $cm.^2$ per g. of coal was calculated from equation (3a).

The method was found to be simple and quick and to give good reproducibility. The major difficulty was found in obtaining a bed free from air bubbles. When air was present, the bed had a characteristic mottled appearance at the surface of the tube and surface areas were both too high and poorly reproducible. This difficulty was overcome by allowing the coal

sample to soak in boiled-out water for an hour before use, with frequent stirring, and by packing the bed wet. If the coal was well wetted and packed under suction (from a water pump) with a continuous flow of boiled-out water, air bubbles were not found in the bed. The bed was kept completely full of air-free water at all times during the testing.

The instrument was tested by measuring the surface area of a sample of glass spheres of size 100-200 microns, the glass having a density of 2.50 g./cc. A microscope size count was made on the spheres and the surface area calculated as described later. Comparing the two areas gave a mean factor of k_0q^2 in equation (3) of 4.75, with the values from six tests lying always within ±6% of the mean. Carman (12) reviews values of k_0q^2 found for spheres and quotes values from 4.5 to 5.1, with a best value of 4.8. The value found was in good agreement with this, and it was concluded that the apparatus was working satisfactorily.

THEORY

Specific Surface Area of Tested Material--The specific surface area of a coal fraction was calculated from the following formulae, which can be easily derived.

$$d = 5\left(\frac{k_0q^2}{4}\right)^{\frac{1}{2}}\left(\frac{R_1}{R}\right)\left(\frac{1-\epsilon}{\epsilon}\right)\sqrt{\frac{\eta L \log(\ell_2/\ell_1)}{\epsilon t}\,10^5} \qquad (3)$$

$$S_0 = \left(\frac{6}{d}\right)10^4 \qquad (4)$$

where d is the surface area mean spherical diameter of the material in microns, S_0 is the specific surface area in sq. cm. per $cm.^3$ of material, k_0q^2 is a factor which varies with the shape of the pores in the bed, R is the radius of tube A, R_1 is the radius of tube C, ϵ is the porosity of the packed bed, η is the viscosity of water, L is the length of the packed bed, ℓ_1 and ℓ_2 are the pressure differentials across the bed initially and finally in cm. of mercury, and t is the time of flow in seconds. The factor k_0q^2 is 4 for circular pores, 4.8 for a bed composed of spheres and 5 for a bed composed of irregular particles (13). It should be noted that d is only an intermediate step in the calculation of the surface area S_0, and it is not necessary to attach any particular physical significance to it. However, values of d were calculated because these values could be compared with the nominal sieve sizes of the material tested. These values, consequently, gave a ready indication of an unsatisfactory test. S_0 is in no sense a mean of determined dimensions but is a direct measure of surface area. For the irregular particles of ground coal, equation (3) becomes

$$d = 5\sqrt{\frac{5}{4}}\left(\frac{R_1}{R}\right)\left(\frac{1-\epsilon}{\epsilon}\right)\sqrt{\frac{\eta L \log(\ell_2/\ell_1)}{\epsilon t}\,10^5} \qquad (3a)$$

In order to test the accuracy of the apparatus, the specific surface area of a sample of glass spheres was determined by microscope measurement and by the permeability method. The specific surface area by microscope measurement was calculated by using the following equation

$$S_o = 6 \int_0^N \mu_i^2 \, dN_i \Big/ \int_0^N \mu_i^3 \, dN_i \qquad (5)$$

where dN_i is the number fraction of spheres in the microscope diameter range $\mu_i + d\mu$. The integrations were performed graphically by plotting the cumulative number of particles below diameter μ_i against μ_i^2 and against μ_i^3 and finding the appropriate areas under the curves.

b) Calculation of area-to-volume shape factors.

The specific surface areas per $cm.^3$, S_o, of 10 sieve fractions of a coal ground according to the standard Hardgrove test (60 grinding revolutions) were determined. As the percentage weight of coal in any fraction, Δp say, and the density ρ were known, the surface area ΔS of the fraction was calculated from

$$\Delta S = \frac{S_o}{\rho} \cdot \Delta p$$

The cumulative total surface area, S, and cumulative weight p were then calculated from

$$S = \sum \frac{S_o \Delta p}{\rho}$$

$$p = \sum \Delta p$$

When S was plotted against p on semi-log paper, it was found that a smooth, shallow curve was obtained. Then

$$\frac{dS}{dp} = \frac{dS}{d(\log p)} \left(\frac{1}{2.3p} \right) \qquad (6)$$

and values of $dS/d(\log p)$ were obtained from the slope of the curve at any given value of p. The specific surface area per gram at a sieve size μ corresponding to weight p is clearly given by

$$S_\mu = \left(\frac{dS}{dp} \right)_\mu \quad cm.^2 \, g.^{-1} \qquad (7)$$

If ρ_μ is the density of coal of size μ and the shape factor for this size is k_μ from equations (7) and (2)

$$k_\mu = \left(\frac{dS}{dp} \right)_\mu \mu \rho_\mu \qquad (8)$$

It should be noted that k_μ is the shape factor at size μ and is not a mean over a range of sieve sizes. k_μ is independent of the size distribution of the ground coal, whereas any mean value of k would depend on the size distribution between the sieve sizes averaged.

RESULTS

Table 1 gives the analyses of the coals used in the tests. The four coals cover a range from low rank high volatile sub-bituminous coal to high rank low volatile anthracite.

Figure 2 gives the variation in apparent density of the ground coals with size. In general, the value of density determined at a given size varied about the mean line within a range of ±3%. Fortunately, the value of dS/dp in equation (6) is insensitive to small changes in density. The effect of density is mainly the direct proportionality shown in equation (8). The water densities,where determined, were equal to the mercury densities within the limits of accuracy of both methods.

Table 2 gives the size/weight distribution of the four coals ground for the standard 60 revolutions and the specific surface areas of the ground fractions. At least three area measurements were made on each fraction; the values obtained were always within ±3% of the mean and were usually within ±1%.

Figure 3 shows the cumulative surface area of material less than 30 mesh (U.S. standard sieve) plotted against the percentage weight undersize for coal B19426. Similar curves were obtained for the other coals tested. The numerical values of the slope were used to obtain shape factors using equation (6) and (8). Table 3 gives the shape factors at various micron sizes. Over the size range investigated (approximately 40 to 600 microns), the shape factor was found to be constant for a given coal, the determined values varying randomly about the mean within about ±4%. There were marked differences in the shape factors for the four coals investigated, the differences being considerably greater than can be explained on the basis of experimental errors of the various determinations made.

DISCUSSION OF RESULTS

The variation of apparent density of coal with size after grinding is to be expected, since stronger material will tend to collect in the coarser fractions. The stronger material will usually be denser since it will contain more mineral matter and denser, more coalified coal particles. This effect is more marked for the weaker coals for two reasons: a) there is a greater difference between the hardness of the mineral matter and the remainder of the coal and b) the grinding has proceeded to a more advanced stage for the weaker coals (although ground for the same number of revolutions). The concentration of denser material in the coarse fractions is partially counteracted by the larger size material having a greater probability of breakage (14).

It appears unlikely that shape factor is a function of the degree of grinding (at least, over the size range investigated). If it were, the factor

would be expected to vary for different sized fractions because the finer fractions contain material which has been broken several times. It is possible, however, that the shape factor varies from one type of grinding process to another.

An examination of Seyler's coal chart (15) indicates that over most of the coal range, an increase of 1% in the hydrogen content of a coal has an equivalent effect on the volatile matter (dry ash free) of about an 8.5% decrease in carbon content, the percentage being expressed on Parr's basis (16). Therefore, it is proposed that the rank of a coal be expressed by

$$\text{Rank Index} = \%\,C \text{ (Parr's basis)} - 8.5\%\,H \text{ (Parr's basis)} \qquad (9)$$

When the volatile matter contents of coals are plotted against this rank index, the points have a considerably reduced scatter about the mean line over that when percentage carbon content alone is used (17). This is also true when grindability indices are plotted against the proposed index as shown in Figure 4 (16). Figure 4 also shows the shape factors of the four coals tested as a function of the rank index. Although definite conclusions cannot be drawn from four results, it seems probable that the variation in shape factor has a similar relation to the rank of the coals as that found for grindability indices.

The geometric or hydrodynamic area obtained with the liquid permeability apparatus should not be a function of the chemical nature or roughness of the particle surface since the resistance to flow is due to the internal friction of the liquid. Also the mean free path of the liquid molecules is not great enough compared to the flow paths for the phenomena of slip to occur. Consequently, the variation of shape factor implies that coals fracture to different mean shapes depending on their rank. A high shape factor means that the particle is flaky, while shape factors approaching the value of six imply that the particles tend towards spherical or cubical shapes. Thus, on the basis of our limited results, anthracites and low rank sub-bituminous coals have more flaky particles, while the more easily broken bituminous coals tend to have more rectangular shaped breakage products.

It is possible that shape factors also depend to a considerable extent on the petrographic constituents of the coals, since it is known that different macerals have conchoidal, splintery, or irregular breakage (18).

CONCLUSIONS

The geometric-surface-area-to-volume shape factor was found to be constant for a given coal over the size range investigated, approximately 40 to 600 microns. It seems likely that the shape factors of coals are related to their rank in a similar manner to that of their grindability indices. Shape factors were found to vary from 7.2 for a medium rank bituminous coal (17.9% volatile matter, d.a.f.) to 9.4 for a high rank anthracite (4.5%) and 9.6 for a low rank sub-bituminous coal (42.4%).

ACKNOWLEDGEMENTS

We wish to express appreciation to G.C. Williams and R.R. Luckie who assisted in the experimental program. We appreciate the financial support of the Coal Research Board of the Commonwealth of Pennsylvania which made this work possible.

REFERENCES

1. "Crushing and Grinding Bibliography", Department of Scientific and Industrial Research (London), H.M.S.O., 1958, p. 99.

2. Walker, P.L. Jr., Rusinko, F. and Austin, L.G., "Advances in Catalysis", Vol. XI, Chapter on Gas Reactions of Carbon, Academic Press Inc., New York, 1959, in press.

3. Aris, R., Chem. Eng. Sci., 6, 262 (1957).

4. Hawksley, P.G.W., Brit. J. Appl. Phys., Supplement No. 3, 51 (1954).

5. Anderson, Robert B., Hall, W. Keith, Lecky, James A., and Stein, Karl C., J. Phys. Chem., 60, 1548 (1956).

6. Carman, P.C. and Arnell, J.C., Can. J. Res., 26A, 128 (1948).

7. Romer, J.B., Proc. Am. Soc. Test. Mat., 41, 1152 (1941).

8. Skinner, D.G. "Pulverised Fuel Conference", Inst. of Fuel (London), 1947, p. 519.

9. Am. Soc. Testing Materials Standard D409-51, Grindability of Coal by the Hardgrove Method.

10. Washburn, E.W., Proc. Nat. Acad. Sci., 7, 115 (1921).

11. Lakhanpal, M.L., Anand, V.D., and Puri, B.R., Nature, 176, 692 (1955).

12. Carman, P.C., "Flow of Gases through Porous Media", Academic Press Inc., New York, 1956, p. 14.

13. Ibid, p. 36.

14. Austin, L.G., "Breakage Functions of Coal Ground in a Standard Hardgrove Mill", to be published.

15. "Technical Data on Fuel", 5th Ed., British National Committee World Power Conference, 1950, p. 393.

16. Fitton, A., Hughes, T.H., and Hurley, T.F., Inst. Fuel (London), 30, 54 (1957).

17. Austin, L.G. Unpublished Results.

18. Stopes, M.C., Proc. Roy. Soc. (London), 90, 470 (1919).

TABLE 1

ANALYSES OF COALS USED

Coal	B-19447	B-17790	B-19426	St. Nicholas Anthracite
Constituent	As used,%	As used,%	As used,%	As used,%
Moisture	1.5	0.8	0.5	1.6
Ash	16.5	7.8	14.5	9.3
Carbon	65.5(83.5)*	78.8(87.6)*	75.2(90.6)*	84.2(95.5)*
Hydrogen	4.7(5.9)*	4.8(5.1)*	3.9(4.5)*	2.4(2.2)*
Nitrogen	1.1	1.5	1.5	0.85
Sulfur	4.5	1.6	1.8	0.5
Oxygen (by difference)	6.2	4.7	2.6	1.1
Volatile Matter (D.A.F.)	42.4	29.2	17.9	4.5

*Parr's basis

TABLE 2

SIZE-WEIGHT DISTRIBUTIONS AND HYDRODYNAMIC SURFACE AREAS OF SIEVE FRACTIONS FOR COALS GROUND ACCORDING TO THE STANDARD HARDGROVE TEST

Sieve Range U. S. Standard Mesh	B-19447		B-17990		B-19426		S.N.A.	
	p*	S_o**	p	S_o	p	S_o	p	S_o
16 x 30	100		100		100		100	
30 x 35	64.25	178	79.97	138	80.37	132	75.26	166
35 x 50	54.05	235	71.78	217	73.13	192	61.10	211
50 x 70	35.55	403	54.06	307	56.00	296	26.98	378
70 x 100	27.02	565	44.78	439	47.45	408	17.67	552
100 x 120	18.48	710	35.62	598	38.03	502	10.78	670
120 x 140	16.89	865	32.78	714	34.81	684	8.99	786
140 x 170	14.63	1001	28.78	948	31.22	744	7.23	1000
170 x 200	12.95	1171	25.95	1036	28.29	944	6.20	1156
200 x 230	11.17	1403	22.26	1235	24.69	1065	5.03	1398
230 x 325	9.82	1730	20.26	1635	22.48	1355	4.30	1717
Minus 325	7.94		11.14		16.29		3.20	
% Weight lost on grinding	0.66		0.72		0.83		(-0.1)	
Mean Hardgrove Index	52		93		99		30	

*p = % by weight below upper sieve size
**S_o = Surface area per unit volume of coal in size range given, $cm.^2/cm.^3$

TABLE 3

SURFACE AREA TO VOLUME SHAPE FACTORS FOR COALS
GROUND ACCORDING TO STANDARD HARDGROVE TEST

B-19447			B-17990			B-19426			St. Nicholas Anthracite		
μ *	$\frac{dS}{dp}$ **	k ***	μ	$\frac{dS}{dp}$	k	μ	$\frac{dS}{dp}$	k	μ	$\frac{dS}{dp}$	k
47.5	1421	9.6	44	1420	7.9	44	1240	7.1	47.5	1340	9.6
62	1124	9.6	62	1040	8.1	62	900	7.3	62	995	9.4
74	935	9.5	74	850	8.0	74	809	7.3	74	850	9.6
88	782	9.5	88	726	8.0	88	632	7.3	88	690	9.3
105	678	9.8	105	610	8.2	105	535	7.4	105	591	9.5
125	565	9.7	125	480	7.8	125	486	7.2	125	475	9.2
138	497	9.6	149	396	7.9	149	357	7.1	149	406	9.4
220	338	9.8	220	268	8.0	210	250	7.2	210	286	9.4
297	230	9.4	297	197	8.0	297	173	7.1	297	201	9.3
500	140	9.6	500	128	8.3	500	100	7.1	500	113	8.9
590	118	9.6	590	104	7.9	590	87.7	7.35	590	101	9.3
Mean k		9.6			8.0			7.2			9.3

* μ is sieve size in microns

** $\frac{dS}{dp}$ is the specific surface area in $cm.^2$ per g. at size μ

*** k is volume-to-surface area shape factor

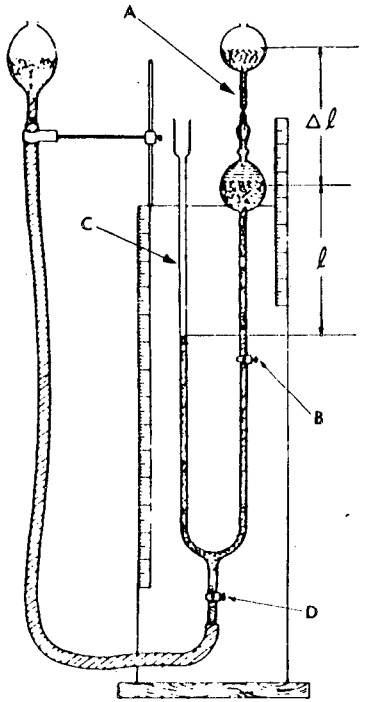

Fig. 1. DIAGRAM OF PERMEABILITY APPARATUS.

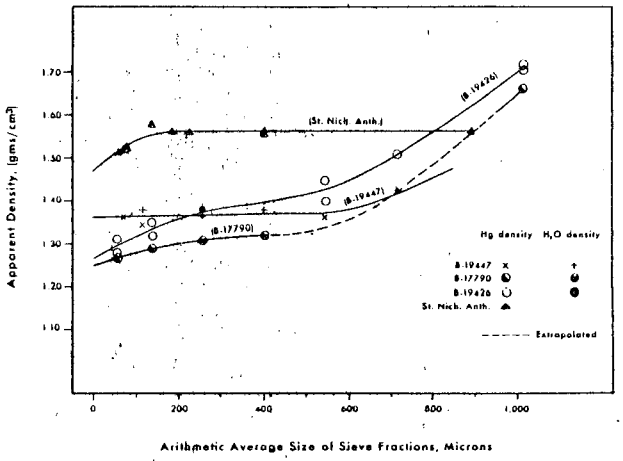

Fig. 2. APPARENT DENSITIES OF SIEVE FRACTIONS OF COALS GROUND ACCORDING TO STANDARD HARDGROVE TEST.

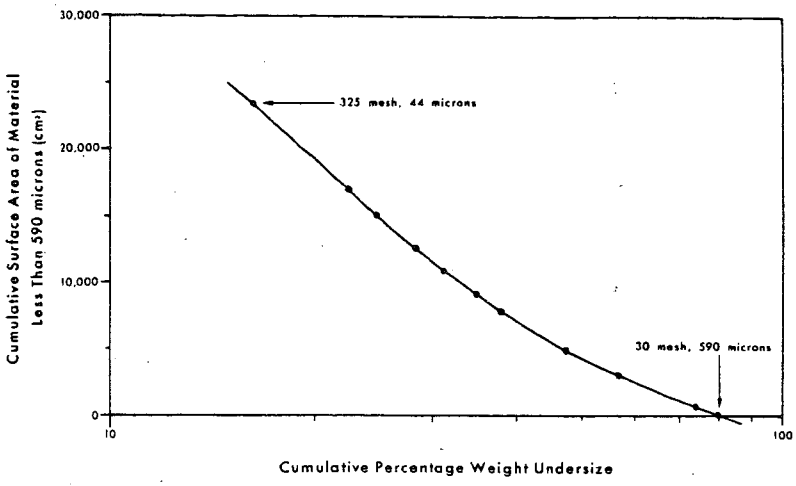

Fig. 3. CUMULATIVE SURFACE AREA AGAINST PERCENTAGE UNDERSIZE FOR COAL B-19426 GROUND ACCORDING TO STANDARD HARDGROVE TEST.

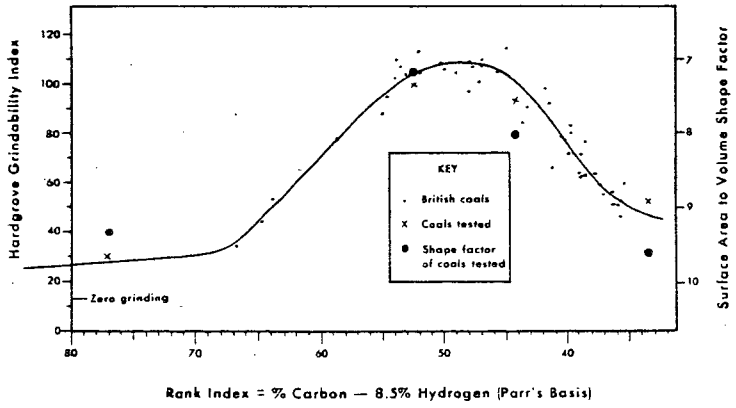

Fig. 4. GRINDABILITY INDEX AND SHAPE FACTOR AS A FUNCTION OF COAL RANK.

Not for Publication
Presented Before the Division of Gas and Fuel Chemistry
American Chemical Society
Atlantic City, New Jersey, Meeting, September 13-18, 1959

The Relation of Microscope Size to Sieve Size for Ground Coals

L.G. Austin, R.P. Gardner, and P.L. Walker, Jr.
Fuel Technology Department, The Pennsylvania State University
University Park, Pennsylvania

INTRODUCTION

The weight versus size distribution of a ground coal is an important parameter in many industrial processes, and there has been much study of such distributions (1). The simplest and most commonly used method of size analysis is sieve analysis, but the finest sieve which can be used with any degree of accuracy has a nominal aperture of 44 microns (U.S. standard sieve No. 325). For material below this size it is necessary to use less direct methods such as air elutriation, sedimentation velocities, and microscopic measurement (2). In the sub-sieve range down to 1 micron, measurement with an optical microscope is simple, avoids problems of agglomeration found with other methods, and gives results which are fairly reproducible. Although microscope counting and measurement is tedious, if two experienced personnel work together, results can be obtained at least as quickly as with most other methods.

To extend a sieve size distribution to sub-sieve sizes, it is necessary to know the relation between sieve size and the particular size property measured in the sub-sieve range. In the case of microscopic measurement, the size property is some characteristic visual dimension. The most commonly used dimension is the "projected area diameter", that is, the diameter of the circle which has the same area as the projected outline of the particle in the plane of the microscope slide. In the work described in this paper, the relation between microscope diameter (defined as above) and sieve size is investigated.

REVIEW OF PREVIOUS WORK

Skinner, Boas-Traube, Brown, and Hawksley (3) measured the ratio of microscopic diameter to sieve size for coal which just passed a 7-mesh sieve. They obtained a mean ratio of 1.42. They state that it is not known whether this ratio varies with size. Heywood (4) investigated this ratio for a number of different materials and found values between 1 and 1.8, depending on the geometric shape of the particles. He has also proposed (5) an empirical formula which gives this ratio as a function of m and n, where m is the microscopic breadth of the particle divided by its thickness and n is the breadth divided by the length. Heywood states (6) that the relation between microscope diameter and sieve size is dependent only on the geometry of the particles and not on their size. Guruswamy and co-workers (7) measured the ratio of microscope diameter to sieve size for a series of sieve fractions of a coal which had been broken upon being dropped on to a metal plate. The ratio appeared to increase slightly with decrease in size over a range of approximately 3000 to 100 microns sieve size, the ratio having a mean value of about 1.5.

APPARATUS AND EXPERIMENTAL TECHNIQUE

Microscopic size counts were performed on a number of sieve fractions of coal in the range of 30 to 325 U.S. standard sieve sizes. The measurements were made by projecting the field on to a ground glass screen on which circles of varying radii were drawn; the field was then moved to bring each particle under the appropriate diameter circle. By calibration with a microscopic scale, the representative size of the circles for a given magnification was known. Each particle was assigned on an area basis to a group lying between two circles. From such a count, the cumulative percentage number of particles below any given microscope size was obtained.

For sieve fractions below 170 mesh, slides were prepared in the following manner. A sample of the coal was stirred vigorously in several ml. of toluene until well dispersed, and a drop of the suspension was transferred to 1 ml. of a 10% ethyl cellulose in toluene solution. After stirring, a drop of this suspension was spread on a slide and allowed to thicken. Using this technique, extremely uniform and well dispersed fields were obtained. For larger sizes, it was found that the particles tended to project from the dried cellulose layer; and it was not possible to get clear images of such particles. Consequently, dry slides were prepared by tipping a small amount of the sieve fraction on to the slide and spreading the particles with a fine brush. For these sizes, agglomeration did not occur to any significant extent.

The coals tested were ground according to the standard Hardgrove test (8), as described in a previous paper (9).

THEORY

Let the external geometric surface area and the volume of the particle of sieve size μ be given by

$$S = k_1 \mu^2$$

and

$$V = k_2 \mu^3.$$

Then

$$dS = k_1 \mu^2 dN$$

and

$$dV = k_2 \mu^3 dN$$

where dN represents the number of particles of size $\mu + d\mu$. Over a short size range, k_1 and k_2 may be assumed to be constant and

$$\frac{S}{V} = \frac{k_1}{k_2} \frac{\int \mu^2 dN}{\int \mu^3 dN}.$$

Now $S/V = S_o$, the specific surface area of the material; and if a shape factor k is defined by $k = S_o\mu$, then $k = k_1/k_2$. Therefore,

$$S_o = k \frac{\int \mu^2 dN}{\int \mu^3 dN}.$$

Defining R by $R = d_p/\mu$, where d_p is the projected area diameter,

$$R = \frac{S_o}{k} \frac{\int_0^N d_p^3 dN}{\int_0^N d_p^2 dN} . \qquad (1)$$

For the size fractions and coals investigated, S_o and k were known from previous determinations (9). The integrals were evaluated graphically.

Although Equation (1) is derived without recourse to the concept of mean values, k/S_o is a specific-area (geometric area per unit volume) mean-sieve size, while $\int d_p^3 dN / \int d_p^2 dN$ is a specific-area-mean-microscope size. Thus, Equation (1) can be given as

$$R = \frac{\tilde{d}_p}{\tilde{\mu}} \qquad (1a)$$

where $\tilde{\mu}$ is a specific-area-mean-sieve size and $\tilde{d}_p$ is specific-area-mean-microscope size. In general, it was found that, within two or three per cent,

$$\tilde{d}_p \simeq \left(\frac{\int_0^{100} d_p^2 dN}{100} \right)^{\frac{1}{2}} \simeq \left(\frac{\int_0^{100} d_p^3 dN}{100} \right)^{\frac{1}{3}} . \qquad (2)$$

Thus, the specific-area mean, area mean, and volume mean microscope size were not significantly different.

RESULTS

Table 1 gives the analyses of the coals used. They range from a high rank anthracite to a low rank bituminous coal.

Figure 1 shows the relation between $\tilde{d}_p$ and $\tilde{\mu}$ determined for sieve ranges of 35 x 50, 50 x 70, 70 x 100, 100 x 120, 120 x 140, 140 x 170, 170 x 200, 200 x 230, and 230 x 325 U.S. sieve numbers. For sieve sizes smaller than 80 microns (approximately 170 mesh), the ratio R appears to be constant at 1.68, with no significant difference between the coals tested. For sieve sizes larger than 80 microns, however, the curve bends over sharply, giving a second straight line section which does not pass through the origin. The variability of the results tends to obscure any differences between the coals. The best-fit curve above a sieve size of 80 microns has the equation

$$d_p = 40 + 1.18\mu \qquad (3)$$

or

$$\mu = \frac{d_p - 40}{1.18} . \qquad (3a)$$

The disadvantage of using $\tilde{\mu}$ to correlate with $\tilde{d}_p$ is that any error in measurement of the specific surface, S_o, of the sieve fraction considered will reflect as an error in $\tilde{\mu}$. This is in addition to the error involved in microscopic measurements, which gives rise to inaccuracies in the $\tilde{d}_p$ values. If the arithmetic mean sieve size of the fraction is used, the surface area error is avoided, but no allowance is made for the size distribution within the fraction. Figure 2 shows the relation between the volumetric-mean microscope diameter (which is close in value to $\tilde{d}_p$, see Equation (2)) and the arithmetic mean sieve size. The general form is the same as Figure 1, but there appears to be significant differences between coals for the portion of the curve above 80 microns.

Figure 3 gives values of R as a function of microscope size for the best fit curves of Figures 1 or 2. Values of sieve size calculated using these values of R and measured microscope diameters lie within ±10% of the arithmetic mean sieve sizes for all the results obtained.

DISCUSSION OF RESULTS

Previous results (9) indicated no change in the shape factor k with size for a given coal in the range 40 to 600 microns, yet R decreased significantly above sieve sizes of 80 microns. This result appears to be in conflict with Heywood's prediction (6). Further, the values of R obtained for the larger sizes were lower than those reported by other workers (3,7).

The material below 170 mesh size was viewed in ethyl cellulose suspension; but it would be expected that this would tend to reduce R rather than increase it, since the thinner sides of the particles might lie in the line of sight. It is clear that the curve of d_p against μ must pass through the origin. Therefore, even if the minus 170 mesh results were not available, it would be predicted that the curve must bend towards the origin. The shape of the curve is not caused by errors in area measurements, since Figure 2 is substantially the same even though surface area measurements play no part in its compilation.

It would appear that the method of size reduction of the particles has a considerable influence on the values of R, since the values obtained by Guruswamy and co-workers (7) were significantly higher than the results presented here. It would also appear that, for the narrow size ranges used, the use of a volume-mean microscope diameter and an arithmetic-mean sieve size is at least as satisfactory as using specific area mean diameters.

Although the coals used had specific-surface-area-shape factors, k, differing by as much as 30% (9), a significant correlation between the values of R and k was not clear. A possible explanation for this is as follows. If the ground coals have about the same length and breadth ratio, n, but varying thickness to breadth ratios, m, then it is easily shown that the values of k may vary widely with a comparatively small change in R. For instance, assuming a rectangular prism shape with n = 2 and m varying from 1/0.3 to 1/0.5 (10), k will vary by almost 30% while R will vary by less than 10%.

It is fortunate that the extrapolation of the curves of Figures 1 and 2 to the origin gives a constant value of R for the sub-sieve fraction, since this is the size range of most significance. The use of a value of R of 1.68 enables sub-sieve microscope distributions to be joined on to the sieve size distribution, in the present work, where the coals were ground in a Hardgrove machine.

CONCLUSIONS

For coals ground in the standard Hardgrove test mill, the ratio of microscope "projected area" diameter to sieve size, for material finer than 170 U.S. sieve size was found to be 1.68 for all the coals tested. Above this size, the ratio appears to decrease with increasing size to a limiting value of about 1.2. Although there may be a significant variation of the values of R (at the larger sizes) with the type of coal ground, this variation appears to be less than ca. ±10% for the four coals tested.

ACKNOWLEDGEMENTS

We wish to express appreciation to G.C. Williams and R.R. Luckie who assisted in the experimental program. We appreciate the financial support of the Coal Research Board of the Commonwealth of Pennsylvania which made this work possible.

REFERENCES

1. "Crushing and Grinding Bibliography", Department of Scientific and Industrial Research (London), H.M.S.O., 1958, p.18.
2. Jarrett, B.A. and Heywood, H., Brit. J. Appl. Phys., Supplement No. 3, S 21 (1954).
3. Skinner, D.G., Boas-Traube, S., Brown, R.L., and Hawksley, P.G.W., "Determinations of Particle Size in Sub-Sieve Range", The British Colliery Owners Research Association and The British Coal Utilisation Research Association, 1954.
4. Heywood, H., "Chemical Engineering Practice", Vol. 3, Butterworths' Scientific Publications, 1957, p.40.
5. Heywood, H., Trans. Instn. Chem. Engrs. (Supplement) 25, 14 (1947).
6. Reference 4, p.42.
7. Guruswamy, S., Roy, L.C., Das Varma, R.L., and Srinivasan, S.R., J. Sci. Industr. Res. (India) 12B, 91-105 (1953).
8. Am. Soc. Testing Materials Standard D409-51, Grindability of Coal by the Hardgrove Method.
9. Austin, L.G., Gardner, R.P., and Walker, P.L. Jr., The Geometric Area Shape Factors of Coals Ground in a Standard Hardgrove Mill, presented before the Gas and Fuel Division at the September, 1959 meeting of the American Chemical Society.
10. Guruswamy, S., Brit. J. Appl. Phys., Supplement No. 3, S 81 (1954).

TABLE 1

ANALYSES OF COAL USED

Coal	B-19447	B-17790	B-19426	St. Nicholas Anthracite
Constituent	As used,%	As used,%	As used,%	As used,%
Moisture	1.5	0.8	0.5	1.6
Ash	16.5	7.8	14.5	9.3
Carbon	65.3(83.5)*	78.8(87.6)*	75.2(90.6)*	84.2(95.5)*
Hydrogen	4.7(5.9)*	4.8(5.1)*	3.9(4.5)*	2.4(2.2)*
Nitrogen	1.1	1.5	1.5	0.85
Sulfur	4.5	1.6	1.8	0.5
Oxygen (by difference)	6.2	4.7	2.6	1.1
Volatile Matter (D.A.F.)	42.4	29.2	17.9	4.5
Shape Factor (k)	9.6	8.0	7.2	9.3
Hardgrove Grindability Index	52	93	99	30

* Parr's basis

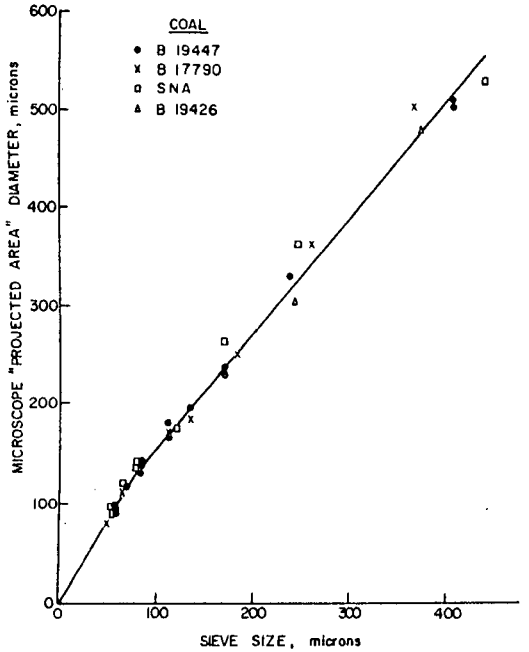

FIG. 1 – Relation between microscope diameter and sieve size for coals ground according to Standard Hardgrove Test.

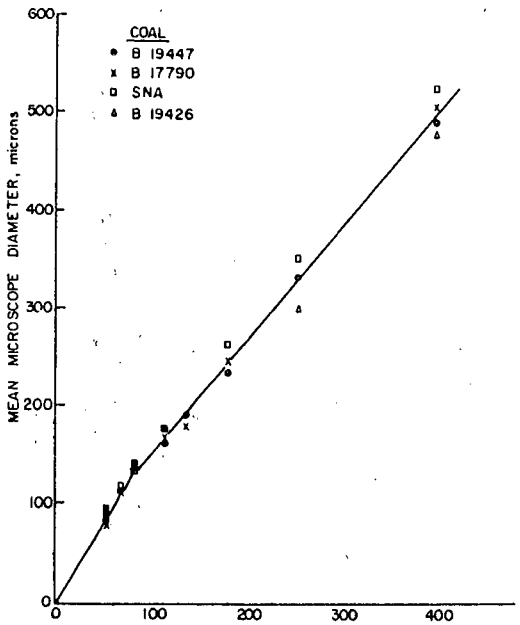

FIG. 2 – Relation of mean microscope size to arithmetic mean size.

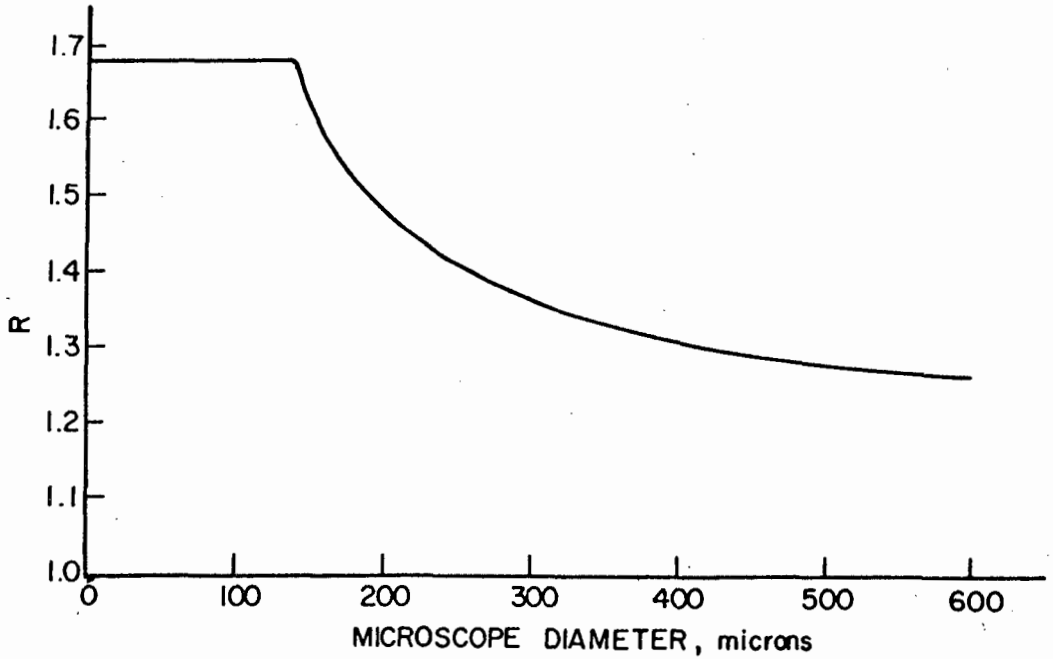

FIG. 3 — Change of microscope-size-to-sieve-size ratio (R) with microscope size for coals ground according to the Standard Hardgrove Test.

Not for Publication

Presented Before the Division of Gas and Fuel Chemistry
American Chemical Society
Atlantic City, New Jersey, Meeting, September 13-18, 1959

The Production of Fresh Surface during the Grinding of Coal in a Standard Hardgrove Mill

L.G. Austin, R.P. Gardner, and P.L. Walker, Jr.
Fuel Technology Department, The Pennsylvania State University
University Park, Pennsylvania

INTRODUCTION

For many years there has been considerable discussion as to whether the energy per unit volume required for size reduction of brittle materials is (a) proportional to the fresh area produced (Rittinger's Law) or (b) proportional to the reduction in volume of the particles (Kick's Law). Bickle (1) has given an excellent review of the available literature. For fine grinding, Rittinger's Law appears to be the law of most general application. Recent workers (2,3) consider such laws to be of limited utility in problems of mill design and operation. However, the relation of grinding energy to fresh surface area produced is of interest chemically as it offers a method of investigating surface energies of materials (4).

REVIEW OF PREVIOUS WORK

Although Rittinger's Law has been widely investigated for quartz, magnetite, and a variety of ores, there have not been many investigations of the law for coal. The primary reason for this is that coal contains an internal surface area (within micropores) that is large compared to the external area even for finely ground particles (5). Since most methods of area measurement measure, either completely or partially, this internal area, the increase in area upon grinding is obtained as the small difference between two large quantities. Consequently, the results are insufficiently accurate to be of much use.

Hardgrove (6) calculated proportional areas of ground coal from the sieve analysis. He assumed that shape factors and coal density remained constant throughout the size range and that shape factors were the same for different coals. The integration of the size distribution to a proportional area was carried out assuming that the minus 325 mesh size had a mean sieve size of 25 microns. Using these areas, he found the fresh surface produced to be proportional to the number of revolutions of the mill over a restricted range of revolutions. When large amounts of breakage had occurred, the increase in surface area on further grinding was less than that predicted by the increased number of revolutions; and Rittinger's Law did not hold. Hardgrove attributed this behavior to blanketing of the grinding by the fines produced. He defined the grindability of a coal in terms of the increase in surface area produced compared to that of the increase produced on grinding a standard coal the same number of revolutions, 60 revolutions being chosen as a standard condition. Hardgrove later found that there was an empirical relation between the grindability defined in this manner, and the per cent by weight of coal, p, passing a 200 mesh sieve, the relation being

$$\text{Hardgrove Index} = 13 + 3.465\ p. \qquad (1)$$

Romer (7) attempted to overcome some of the obvious objections to Hardgrove's work by measuring the surface areas of ground coals using an air permeability method. This method gave the hydrodynamic or geometric area of the particles. Romer found that the grindability indices calculated using the direct area measurements were considerably different from the Hardgrove indices, the surface areas being much higher than predicted for the products of coals of high Hardgrove indices. He then showed that Rittinger's Law applied when the load on the mill or the number of revolutions of the mill were varied. Thus, any non-applicability of Rittinger's Law in Hardgrove's original work was ascribed to inaccurate surface area measurements. Objections still remain to the surface areas obtained by Romer. The permeability method of area measurement is known to be inaccurate for a sample of mixed sizes in which the largest to finest size ratio is greater than 3 (8). Romer actually measured samples which consisted of coal of size range from one to 44 microns. Also, a certain amount of very fine material is lost during the grinding and sieving operations, and this surface area is not included in the measured area.

Bennet and Brown (2) argue that proofs of Rittinger's Law for coal are of little significance because the fresh surface area produced cannot be measured unequivocally.

EXPERIMENTAL PROCEDURES

Characteristics of Coals used in Tests - Four coals were used, ranging from an anthracite of 4.5% volatile matter to a low rank bituminous coal of 42.5% volatile matter and 6.2% oxygen content. The analyses were performed on the 16 x 30 mesh coal* which was the starting material for all tests. The proximate and ultimate analyses were carried out according to A.S.T.M. standard procedures.

Preparation of Coal Samples - Since the interest was in the properties of the coal actually used and not in those of the bulk sample supplied, no studies were made on differences in character between the bulk sample and the final sample. The sample for use was prepared from minus 1/2-in. material by passing it through a jaw-crusher followed by a disc mill and sieving out the 16 x 30 mesh fraction on a Rotap sieving machine. The 16 x 30 mesh fraction was removed after each pass through the jaw crusher or disc mill. Microscopic examination showed the sample to be almost free from adhering fines or agglomerates. Before use, the coals were spread on trays in a thermostatically controlled (to ± 0.5°C.) laboratory and allowed to reach equilibrium with the atmosphere. Grinding and weighing were performed in this laboratory.

Grinding of Coal - The coals were ground in a standard Hardgrove test machine according to the A.S.T.M. standard method (9), both to measure the grindability and to provide sufficient fractions of material for surface area measurement. Two of the coals were also ground for varying revolutions of the machine, ranging from 3 revolutions, to 140 revolutions. In every test, 50 g. of coal were charged to the machine and the product sieved, as described below.

Sieving of the Ground Coal - It was considered essential that good performance of sieving be obtained; therefore, a standard procedure was carefully followed in each case. The material from the mill was carefully brushed out into the top sieve of a series of 6 sieves (16 mesh to 120 mesh). The sieves were shaken in

---

* All sieve numbers refer to U.S. standard mesh.

a Rotap sieving machine for 10 minutes, the material through 120 mesh removed, the sieve cleaned if necessary, and the sieves reshaken for five minutes. This was repeated for five minute intervals until the amount of minus 120 mesh material coming through was small. (A total sieving time of 25 minutes was always sufficient). The same procedure was then followed using the minus 120 mesh material in another series of 6 sieves (120 to 325 mesh). The sieves required cleaning more frequently and a maximum sieving time of 35 minutes was sometimes required. Cleaning was carried out by separating the sieves a small amount, inserting a brush and brushing the underside of the top screen. The collected sieve fractions were weighed to the nearest 0.01 g.

It was found that this series of multiple sievings gave weight losses outside of the tolerance given in the A.S.T.M. standard. Therefore, for standard Hardgrove Index determinations, the ground coal was sieved through a 200 mesh sieve only and the multiple sieving performed after the initial weighings. When this was done, the weight loss in the single sieving operation was within tolerance; and if the weight loss in the multiple sieving was assumed to be of material below 200 mesh, the Hardgrove Index was the same as that for the single sieving, within the tolerance allowable (± 2%).

When the coal was ground for a few revolutions only and the amount of fine material formed was small, the minus 120 mesh material was sieved through tared 3 inch diameter sieves. The coal sample plus sieve was then weighed directly to the nearest 5 milligrams

Surface-Area Shape Factors and Apparent Density of Coal Fractions - The shape factors and densities of ground coal fractions were determined as described in an earlier paper (10).

Size Distributions of Sub-Sieve Fractions of Ground Coal - To extend the cumulative weight versus sieve size to sub-sieve size particles, 0.5 g. of the minus 325 mesh fraction was sedimented into a fine and a coarse fraction and microscope sizing carried out on each fraction. The "sinks" obtained after repeated sedimentation with a 1/2 hour settling period were found to be free from any appreciable quantity of fine material. The "floats" were filtered, dried and weighed. Slides of each fraction were prepared and microscopic counts were performed on each fraction, as described in an earlier paper (11). The magnifications used were x 100 on the "sinks" and x 600 on the "floats". The sink material had microscope diameters mainly from 10 to 80 microns in size, and the float material ranged in size from less than 0.8 microns to about 20 microns. A cumulative weight against size distribution was calculated (see theory) for each fraction; and since the respective weight of each fraction was known, a combined distribution could be calculated. Microscope diameters were converted to sieve sizes using the correlation found previously (11).

THEORY

Calculation of Weight Versus Sieve Size Distributions for Sub-Sieve Coal Fraction from Microscopic Measurements - From microscopic count measurements, the cumulative per cent number of particles, N, below a given microscope size was determined as a smooth function of microscope size, d_p. By plotting N against d_p^3, the percentage weight p below a given size d_p was obtained graphically

since

$$\left(p\right)_{d_p} = 100 \frac{\int_0^{d_p} d_p^3 \, dN}{\int_0^{100} d_p^3 \, dN} \qquad (2)$$

This assumes, of course, that the weight of a particle is proportional to the cube of its microscope diameter, but this assumption appears to be justified (12). The microscope size was then converted to sieve size by dividing by 1.68 (11).

Compilation of Accurate Sieve Size Versus Percentage Weight Undersize Curves - When experimental results of weight versus size for varying revolutions were plotted, the results were not very consistent. This was due to the inherent variability of the grinding and sieving operations and inaccuracies in sieve sizes. The results were made more consistent by cross plotting the percentage weight below a given size against revolutions of grinding, drawing the best fit curve to the points, and taking values from the curve for a replot of weight versus size. This technique was found to give a very consistent family of curves, which could be extrapolated accurately to sub-sieve sizes.

Surface Area Change on Grinding - The surface area of ground coal was determined from the percentage weight versus size distribution, the values of shape factor k, and the density of the coal. If p is the percentage by weight below size μ, then the experimental data on size distribution may be expressed graphically in the form, $p = F(\mu)$. As shown (10), $dS = d_p \, k/\mu\rho$. Therefore, the hydrodynamic area of coal between μ_1 and μ_2 is given by

$$S_{\mu_2-\mu_1} = \int_{\mu_1}^{\mu_2} \frac{k}{\mu\rho} \, dp \qquad (3)$$

or

$$S_{\mu_2-\mu_1} = 2.3 \int_{\mu_1}^{\mu_2} \frac{kp}{\mu\rho} \, d(\log p) \qquad (4)$$

From the experimental values, log p can be plotted against log μ; and p, μ, and log p may then be obtained for any value of μ. Since k and ρ are also known for this size, $kp/\rho\mu$ may be plotted against log p and S determined from the area under the curve.

Alternatively, if

$$\frac{d(\log p)}{d(\log \mu)} = n \qquad (5)$$

then

$$S_{\mu_2-\mu_1} = 2.3 \int_{\mu_1}^{\mu_2} \frac{kpn}{\mu\rho}\, d(\log\mu) \qquad (6)$$

This is somewhat more convenient as it allows a direct integration between any required sieve sizes. The values of n for any value of log μ are determined by taking the slope of the log p/log μ distribution plot at that point. Below sieve sizes of 200 microns, n was found to be constant.

Over the part of the distribution for which n is a constant

$$p = B\mu^n \qquad (7)$$

where n and B may be determined from the slopes and intercepts of the curve.

Now

$$S_{\mu_2-\mu_1} = \int_{\mu_1}^{\mu_2} \frac{k}{\mu\rho}\left(\frac{dp}{d\mu}\right) d\mu$$

(sq. meters when μ is in microns)

But from (7), $dp/d\mu = Bn\mu^{n-1}$.

Therefore,

$$S_{\mu_2-\mu_1} = \int_{\mu_1}^{\mu_2} \frac{kBn}{\rho}\mu^{n-2}\, d\mu$$

When k and ρ are constant,

$$S_{\mu_2-\mu_1} = \frac{kBn}{\rho(1-n)}\left[\frac{1}{\mu_1^{1-n}} - \frac{1}{\mu_2^{1-n}}\right] \qquad (8)$$

Kick's Law Calculations - Kick's Law may be expressed in the form (13)

$$E = C \ln\left(\frac{\mu_1}{\mu_2}\right) \qquad (9)$$

where E is the energy per unit weight required to reduce material of size μ_1 to size μ_2, and C is a constant for a given material and process. If material of size μ_1 is broken to a distribution of sizes, the energy required to produce a weight dp of material of size $\mu + d\mu$ is given by

$$dE = C \ln\left(\frac{\mu_1}{\mu}\right) dp \qquad (10)$$

Therefore, the total energy is given by

$$E = C \int_{p=0}^{p=100} \ln\left(\frac{\mu_1}{\mu}\right) dp \qquad (11)$$

It can readily be shown that when the energies required for various size reductions from the same starting material are to be compared, the precise value of μ_1 is not too important. Therefore, it was assumed that the 16 x 30 mesh starting material had a mean size μ_1 of 900 microns. Comparative values of E were obtained for various revolutions of grinding by plotting log $900/\mu$ against p (using the appropriate size distribution of the product) and integrating graphically. The areas were not significantly different when lower size limits of 1 or 0.1 micron were assumed.

RESULTS

Table 1 gives the analyses of the coals tested. Figure 1 shows the size weight distributions of coal B-19447, after correcting the results as described previously. The points in Figure 1 are very consistent and the distribution curves can be drawn with considerable precision. If the straight line portions of the curves are extrapolated and the values of n and B (see Equation 7) determined, then the results are again very consistent, as can be seen from Figure 2.

Table 2 gives the cumulative weight versus microscope size (and corresponding sieve size) calculated using Equation (2), expressed both as a percentage of the minus 325 mesh sample tested and as actual weight of the minus 325 sample. The weight loss on grinding (60 revolutions) and sieving was 0.66 g. per 100 g., and it was assumed that this loss was in the very fine material. It was added, therefore, to the cumulative weight down to 1.5 microns.

Figure 3 shows a complete sieve size-weight distribution for the coal tested, using a factor of 1.68 to convert microscope size to sieve size (11). It can be seen that over the range 3 to 300 microns, the distribution is a straight line on the log-log plot. This type of distribution has been noted previously (14,15,16) and extended below sieve sizes by air elutriation. Rosin and Rammler (17) used air elutriation to extend results to sub-sieve sizes and concluded that the distribution obeyed the Rosin-Rammler law. However, for small sieve sizes, the Rosin-Rammler distribution becomes the simple power distribution found in Figure 3. (In fact, a size distribution of broken coal (18) over a range of 0.004 to 5 inches which fits a Rosin-Rammler plot, also fits a log p-log μ plot over most of the same range). The departure of the curve from the straight line below three microns is almost certainly due to the assumption that all of the weight loss on grinding is less than 1.5 microns. The break in the curve suggests that the weight loss is in sizes of about three microns (sieve size) and less.

Figure 4 shows the surface areas of the ground coal fractions for coal B-19447 calculated using Equations (4), (5), and (8). The surface areas were

calculated assuming that the straight line part of the log p versus log μ distribution (Figure 3) could be extrapolated to a lower limit of 1, 0.1, or 0.01 micron. It was also assumed that the shape factor (a constant in the range from 40 to 600 microns (10)) was constant down to the lower size limit. It is clear that the lower size limit which is chosen considerably affects the absolute value of the surface area. The curve is a straight line when a lower size limit of about 1 micron is used. For the lower size limits of 0.1 and 0.01 micron, the area increases more with revolutions of grinding than Rittinger's Law would predict. Another feature of interest is that the extrapolation of the curves to zero revolutions gives an initial surface area of unground material of 1.2 $m.^2$/100 g. whereas the actual unground surface area is 0.8 $m.^2$/100 g. It appears that an initial small amount of grinding produces 0.4 $m.^2$ of surface area per 100 g. in addition to the 0.117 $m.^2$/100 g./revolution produced for the remainder of the grinding process.

Figure 5 shows the surface area change with grinding for coal B-17790, where a lower limit of 1 micron has been used. After an increase to about 16 $m.^2$/100 g., it appears that the increase in surface area is no longer proportional to the revolutions of grinding. Extrapolation of the straight line portion of the curve to zero revolutions again indicates an initial area of 1.2 $m.^2$/100 g. instead of the expected value of 0.8 $m.^2$/100 g.

Table 3 gives the surface areas from 1 micron to 1190 microns for the four coals ground according to the standard Hardgrove test and also gives the increase in surface areas on grinding. For coal B-19426 and the St. Nicholas anthracite, the results are based on measurements at 60 revolutions only; the cross plotting technique was not used as the data were not available.

Figure 6 gives the increase in E (Equation 11) with revolutions of grinding for coal B-19447. It can be seen that E is not proportional to revolutions of grinding over wide ranges of grinding. Therefore, Kick's Law does not appear to hold for grinding in accordance with the standard Hardgrove test.

DISCUSSION OF RESULTS

Rittinger's Law cannot in general be true, which can be seen if an extreme case is considered as follows. Let a grinding machine be grinding particles which have such strength that the grinding forces imparted by the machine do not exceed this strength. Work will be done without the production of fresh surface, but the material does not have an infinite strength, since a heavier machine would produce breakage. If no change of state of the material occurs, then the energy input is dissipated in a variety of ways. There will be the loss of energy as frictional slip over the surface of the ground material. Also, particularly for ball mills, forces will be transmitted through the material to deliver blows on the mill structure; and energy will be lost as heat of impact and impact waves. In both of these cases, the energy finally appears mainly as heat. In addition, when the ground material fractures, energy will be used to break force bonds across the fresh surface produced and to form internal cracks and flaws. Energy will also be liberated as heat of fracture.

The process of fracture may be loosely described in the following manner. When a particle of coal is crushed it must be raised to a strained state before it fractures. (This, in effect, is an activation energy for crushing). Energy is imparted by the grinding forces which are applied over distances corresponding to the deformation of the particle. The coal then breaks at a flaw

or series of flaws in the material, deformation is removed, and fracture waves propagate through the coal producing fresh surface (19). The excess energy of the fracture waves and the energy released on the relaxation of deformation appear eventually as heat of fracture.

From the above discussion it would appear unlikely that there would be a simple relation between the fresh surface produced and the total energy input to the grinding process; there are so many different ways in which the energy can be distributed. It seems plausible, however, to assume that under certain conditions the energy lost as frictional slip and impact is a fixed fraction of the total input. Fresh internal area does not seem to be produced; except, perhaps, in direct proportion to the external area (20). A fracture wave will propagate until it reaches a free surface and it will not end within the material. (Gross and Zimmerly (21) found that for quartz, internal area was broken out on grinding and impact crushing, rather than increased). Thus, if the energy used to produce fresh surface is a fixed proportion of the strain energy, which in turn is a fixed fraction of the total energy input, Rittinger's Law would hold. To investigate the surface to strain energy relation further, a distinction can be made between the "strength" of a coal and its "hardness". The strength is here arbitrarily defined as the strain energy required before a particle fractures (which is a function of the type of forces imparting this energy to the particle). The hardness is arbitrarily defined as the strength of surface bonds in the material. Clearly two particles may have the same composition and hence the same hardness but may have widely different strengths, if one is highly flawed and the other not.

Consider two such particles of similar "hardness" but different strengths. The stronger one will require the addition of more energy to fracture it, but it seems possible that on fracture it will break into many smaller pieces. On the other hand, the weaker particle will break more readily with a lower energy content but will break into fewer pieces with correspondingly lower fresh surface. Similarly, a large impulsive force of low energy application might cause breakage with small area production; whereas a smaller force applied for a much longer time and deformation would produce a larger surface area on eventual shatter. Thus it is possible that particles of entirely different strengths, and hence probabilities of breakage, have breakage functions which automatically compensate, so that the fraction of the strain energy which is used to produce fresh surface is constant. Bickle (22) states that this has been considered theoretically, but gives no reference to such studies. Such a concept would go part way toward explaining the validity of Rittinger's Law with progressive grinding, although the strength of coal particles is known to vary with size (23,24) and degree of grinding. This concept implies that grindability indices based on surface-area increase measure a parameter proportional to hardness rather than a combined effect of hardness and strength. It is interesting to see that there is a pronounced correlation between grindability indices and the Vickers Microhardness test (25).

As particles become smaller and stronger (in comparison to their size) on grinding due to the breaking out of flaws, they may eventually reach a stage where the crushing forces of the machine are insufficient to cause much breakage. Grinding experience indicates that it is extremely difficult to reduce anthracite below 0.1 to 1 micron in size in conventional grinding apparatus. It may be postulated that somewhere near this size range the major flaw structure of the coal has been completely broken out and that grinding is more difficult by an order of magnitude or more. Van Krevelen (26) states that Boddy found coal particles to be initially crushed to 1 micron in size. As the surface area of this material is of the same order as the macropore area of unground coal, Van Krevelen suggests that breakage to 1 micron is favored by the macropore system. For smaller particles, the coal tends to plastically deform rather than fracture;

this implies much greater strength and a low grindability. An alternative hypothesis is that agglomerates of fine particles tend to trap air and on grinding behave somewhat like miniature balloons. The crushing force is applied to the "balloon" and the energy is expended in compressing the contained gas. For grinding in liquid media, the fluid is incompressible and the forces are imparted to the coal particles; it is well known that liquid grinding can be used to produce very fine sizes.

In spite of the theoretical objections to Rittinger's Law, there is considerable evidence that under a restricted range of conditions the Law is closely obeyed. The correlation of the increase in surface area with grinding obtained in this work is not conclusive, since the lower size limit chosen for the integration to obtain surface area is rather arbitrary. Microscopic studies of the fine fractions of ground coal indicated that material below 1 micron in size was not present in large quantities, although there still remains the question of the fineness of the material making up the weight loss on grinding and sieving. From electron micrographs of ground coal, Preston and Cuckow (27) conclude that coals ground in the normal manner had few particles of less than about 1 micron in size. By taking a lower limit of 1 micron, it is not assumed that material less than 1 micron is absent but rather that 1 micron represents an effective lower limit for the straight line log p/log μ distribution extrapolated from the sieving results. The strict linearity, over a fairly wide range of grinding, of the results plotted in Figure 4 for the 1 micron lower limit would hardly occur by coincidence; and it must be concluded that the evidence for the accuracy of Rittinger's Law is quite strong.

Figure 7 shows the Hardgrove Grindability Indices of a number of British coals (15) and the four coals tested in this work, as a function of a rank index (10). It is clear that the grindability characteristics of a coal are closely allied to its rank. Although the British coals (because they are of one geological era) might be expected to form a fairly consistent pattern, the coals used in our experiments fit the mean line with as good an accuracy as the British coals. Deviations from the mean line are quite considerable in some instances, more than would be expected by experimental error of determination of C, H, or Hardgrove Index. This may be due to several causes:

a) The mineral matter of a coal might considerably influence its grindability.

b) Grindability, as measured by the Hardgrove Index, might not be an accurate representation of the grinding strength of the coal.

c) Differences in the amounts of macerals present in the coal might cause considerable change in strength.

d) The grindability might be influenced by factors which do not depend closely on rank, for example flaw structure.

At the moment, it is only possible to discuss cause (b) with knowledge obtained from our own results. Figure 8 shows the per cent by weight less than 200 mesh plotted against surface area for varying revolutions for coals B-19447 and B-17790. Clearly the increase in surface area is not related to p_{200} in the form of Equation (1). The surface area is not linearly proportional to p for coal B-17790, although a straight line could be drawn with a fair degree of accuracy.

Figure 9 shows p_{200} plotted against increase in surface area for the four coals ground for 60 standard revolutions, and it also shows the Hardgrove Index as a function of surface area increase. It can be seen that the Hardgrove Index is not proportional to the increase in surface area. (Surface areas used are

those calculated on the assumptions that the shape factor is constant over the range 1 to 1190 microns and that 1 micron is an effective lower limit; it has only been shown that the shape factor is constant over the range of 40 to 600 microns (10)).

From Figure 9 it can be seen that the increase in surface area is proportional to p_{200} only to a degree of accuracy of about ± 10%. This is of the same order as the deviations of Hardgrove Index values from the best fit curve in Figure 7, and it is possible that part of the deviations are caused by the Hard-Grove Index (which depends on p_{200}) not being an accurate representation of the increase in surface area. This is particularly likely to be true where a coal fractures to give products with an abnormal shape factor, for in this case two coals might have very similar size distributions on grinding but would have considerably different surface areas.

Callcott (28) argues that the increase in surface on grinding is of little significance in practical grinding studies. He analyzes the problem of grinding in the following manner: Given different sized feeds into a grinding machine, what will be the size distributions of the products? Or if different machines operate with different size feeds, how much of the difference in products is due to the different feed sizes and how much is due to differences caused by the machines? Callcott suggests using p as an index of grindability in preference to the Hardgrove Index (this was also suggested by Frisch and Holder (29)). He does not believe that the work on surface area increase during grinding justified the use of any index except a simple index of breakage defined by p. The significance of the grindability index p may be stated in these terms: If a certain coal produces 10 per cent of material below 200 mesh in the standard Hardgrove test and another coal produces 20 per cent, then it is likely that on grinding in an industrial mill, the first coal will have approximately half the throughput of minus 200 mesh material obtained with the second.

Thus, it would appear that p_{200} is a better index of grindability than the Hardgrove Index, both for the reasons given by Callcott and because it is a better index of surface area increase. The Hardgrove Index may be used instead of p_{200}, if it is borne in mind that a Hardgrove Index of 13 represents zero production of fresh surface. For scientific work it is recommended that the index used should be the increase in surface area per revolution of grinding (over the range in which linearity is obtained).

CONCLUSIONS

The log p versus log μ straight line portions of the distributions found for coals ground according to the Hardgrove test can be extrapolated to at least 3 microns sieve size. The weight loss on grinding appears to be mainly material of less than 3 microns sieve size.

For the two coals tested at varying revolutions of grinding, a negligible amount of grinding produced about 0.4 $m.^2/100$ g. of fresh geometric surface; but after this initial abnormal increase, the increase in surface area was proportional to the revolutions of grinding up to the condition of at least 20% of the material through a 200 mesh sieve. This was true when a lower limit of size of about 1 micron was used to calculate the surface area. Kick's Law did not apply. The percentage of material passing a 200 mesh sieve is very approximately proportional to the increase in surface area on grinding. More precise values of surface area increase per revolution of grinding will be obtained in future work, and these values compared to the rank of the coals used.

ACKNOWLEDGEMENTS

We wish to express appreciation to G.C. Williams and R.R. Luckie who assisted in the experimental program. We appreciate the financial support of the Coal Research Board of the Commonwealth of Pennsylvania which made this work possible. We express our gratitude to Messrs. R.M. Hardgrove and J.B. McIlroy of the Babcock and Wilcox Company for supplying coal samples and relevant analyses for our use.

REFERENCES

1. "Crushing and Grinding Bibliography", Department of Scientific and Industrial Research (London), H.M.S.O., 1958, p.1. See also pp. 159-183.
2. Bennet, J.G., and Brown, R.L., J. Inst. Fuel, 14, 135 (1941).
3. Callcott, T.G., ibid, 29, 524 (1956).
4. Sales, H., and Huttig, G.F., Tonind. Ztg. 186 (1954).
5. Anderson, Robert B, Hal, W. Keith, Lecky, James A., and Stein, Karl C., J. Phys. Chem., 60, 1548 (1956).
6. Hardgrove, R.M., Trans. Am. Inst. Chem. Engrs., 34, 131 (1938).
7. Romer, J.B., Proc. Am. Soc. Test. Mat., 41, 1152 (1941).
8. Carman, P.C., "Flow of Gases through Porous Media", Academic Press Inc., New York, 1956, p.36.
9. Am. Soc. Testing Materials Standard D409-51, Grindability of Coal by the Hardgrove Method.
10. Austin, L.G., Gardner, R.P., and Walker, P.L. Jr., The Geometric Area Shape Factors of Coals Ground in a Standard Hardgrove Mill, presented before the Gas and Fuel Division at the September, 1959 meeting of the American Chemical Society.
11. Austin, L.G., Gardner, R.P., and Walker, P.L. Jr., The Relation of Microscope Size to Sieve Size for Ground Coals, presented before the Gas and Fuel Division at the September, 1959 meeting of the American Chemical Society.
12. Heywood, H., "Chemical Engineering Practice", Vol. 3, Butterworth's Scientific Publications, 1957, p.40.
13. Walker, W.H., Lewis, W.K., McAdams, W.H. and Gilliland, E.R., "Principles of Chemical Engineering", McGraw-Hill Pub. Co., 3rd Edition, 1937, p.252.
14. Fuel Research Technical Paper 49, Dept. Sci. Ind. Research (Brit.) (1947).
15. Fitton, A., Hughes, T.H., and Hurley, T.F., J. Inst. Fuel (London), 30, 54 (1957).
16. Callcott, T.G., ibid, 29, 207 (1956).
17. Rosin, P. and Rammler, E., ibid, 7, 29 (1933).
18. Brown, R.L., Reference (1), p. 19.
19. Poncelet, E.F., Trans. Am. Inst. Mining Met. Engrs., 169, 37 (1946).
20. Johnson, J.F., Axelson, J.W., and Piret, E.L., Chem. Eng. Progr., 45, 708 (1949).
21. Gross, J. and Zimmerly, S.R., Trans. Am. Inst. Mining Met. Engrs., 87, 35 (1930).
22. Bickle, W.H., Reference (1), p.5.
23. Millard, D.J., Newman, P.C., and Phillips, J.W., Proc. Phys. Soc., 68B, 723 (1955).

REFERENCES
(contd.)

24. Gaddy, F.L., Bull. Va. Polyt. Inst., 49, Engng. Exp. Sta. Ser. 112 (1956).

25. Van Krevelen, D.W. and Schuyer, J., "Coal Science", Elsevier Publishing Co. 1957, p.274.

26. Ibid, p. 275.

27. Preston, G.D., and Cuckow, F.W., "Ultrafine Structure of Coals and Cokes", Brit. Coal Utilisation Research Assoc., 334 (1944).

28. Callcott, T.G., J. Inst. Fuel (London) 30, 466 (1957).

29. Frisch, M., and Holder, G.C., Combustion, June-July, 29 (1933).

TABLE I

ANALYSES OF COAL USED

Coal	B-19447	B-17790	B-19426	St. Nicholas Anthracite
Constituent	As used,%	As used,%	As used,%	As used,%
Moisture	1.5	0.8	0.5	1.6
Ash	16.5	7.8	14.5	9.3
Carbon	65.3(83.5)*	78.8(87.6)*	75.2(90.6)*	84.2(95.5)*
Hydrogen	4.7(5.9)*	4.8(5.1)*	3.9(4.5)*	2.4(2.2)*
Nitrogen	1.1	1.5	1.5	0.85
Sulfur	4.5	1.6	1.8	0.5
Oxygen (by difference)	6.2	4.7	2.6	1.1
Volatile Matter (D.A.F.)	42.4	29.2	17.9	4.5
Shape Factor (k)	9.6	8.0	7.2	9.3
Hardgrove Grindability Index	52	93	99	30

* Parr's basis

TABLE 3

HYDRODYNAMIC SURFACE AREAS OF COALS GROUND ACCORDING TO THE STANDARD HARDGROVE TEST

Coal	Hardgrove Grindability Index	Surface Area ground coal $m.^2/100$ g.	Increase in Surface Area $m.^2/100$ g.	Rank-Index of coal % C - 8.5 % H
B-19447	52	7.6	6.8	33.5
B-17790	93	15.9	15.1	44.2
B-19426	99	14.5	13.7	52.4
St. Nicholas anthracite	30	3.4	2.6	77.0

TABLE 2

SIZE DISTRIBUTION BELOW 325 MESH OF COAL B-19447 GROUND ACCORDING TO STANDARD HARDGROVE TEST

Microscope diameter, microns	Equivalent sieve size, microns	Cumulative % by weight of -325 fraction tested	Cumulative weight expressed as a % of total coal ground	Plus 0.66% weight loss of fine material on grinding
0	0	0	0	
0.7	0.4	0.0046	0.00035	
0.9	0.5	0.014	0.00104	
1.3	0.8	0.049	0.00356	
1.8	1.0	0.15	0.0108	
2.6	1.6	0.56	0.0408	(0.701)
3.5	2.1	1.24	0.090	(0.750)
4.4	2.6	2.18	0.16	(0.819)
5.8	3.5	3.67	0.27	0.927
7.3	4.3	6.00	0.44	1.10
8.8	5.2	8.51	0.62	1.28
10.2	6.1	9.90	0.72	1.38
13.1	7.8	14.7	1.07	1.73
21.0	12.5	29.2	2.12	2.78
26.2	15.6	36.1	2.62	3.28
35.0	20.8	44.9	3.26	3.92
43.6	26.0	56.0	4.07	4.73
52.5	31.0	70.6	5.14	5.80
61.0	36.4	83.8	6.10	6.76
70.0	41.6	93.7	6.82	7.48
78.6	47.0	100.0	7.28	7.94

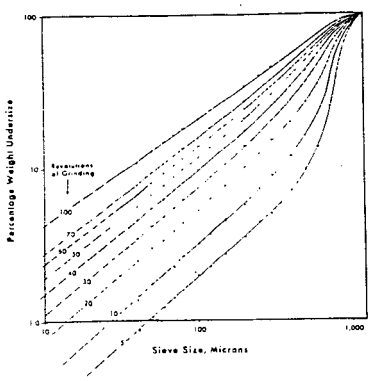

CORRECTED PERCENTAGE WEIGHT UNDERSIZE VERSUS SIEVE SIZE DISTRIBUTIONS FOR COAL B-19447

Figure 1

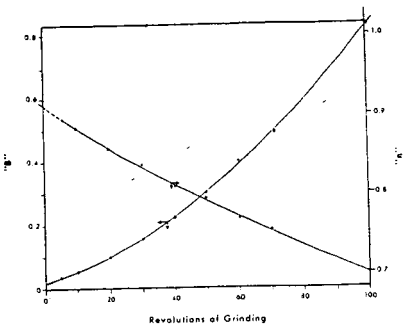

VALUES OF "n" AND "B" IN $p = B\mu^n$ FOR COAL B-19447 GROUND FOR VARYING REVOLUTIONS

Figure 2

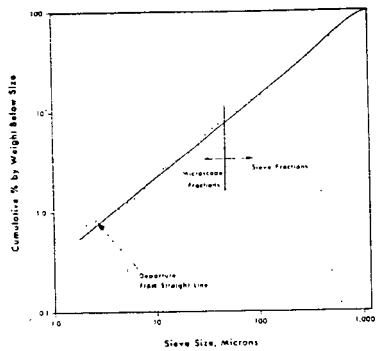

EXTENDED PERCENT WEIGHT UNDERSIZE VERSUS SIEVE SIZE DISTRIBUTION FOR COAL B-19447 GROUND FOR 60 REVOLUTIONS

Figure 3

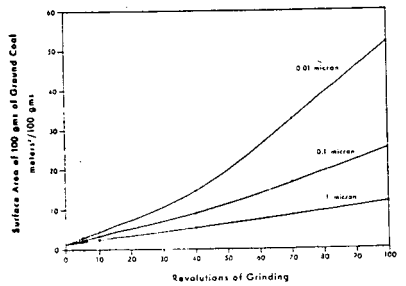

INCREASE OF HYDRODYNAMIC SURFACE AREA OF GROUND COAL WITH REVOLUTIONS OF GRINDING FOR COAL B-19447, ASSUMING 1, 0.1 AND 0.01 MICRONS AS THE SMALLEST SIZE PRESENT

Figure 4

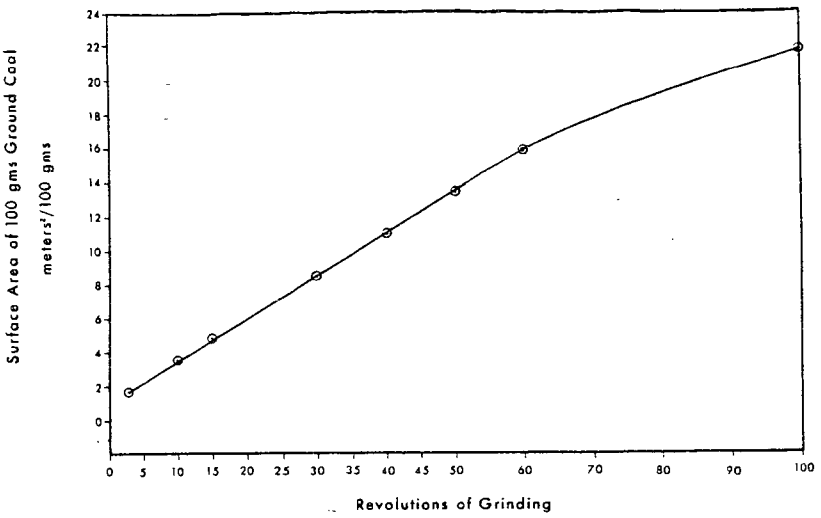

INCREASE OF HYDRODYNAMIC SURFACE AREA OF GROUND COAL WITH REVOLUTIONS OF GRINDING FOR COAL B-17790, ASSUMING 1 MICRON AS LOWER LIMIT

Figure 5

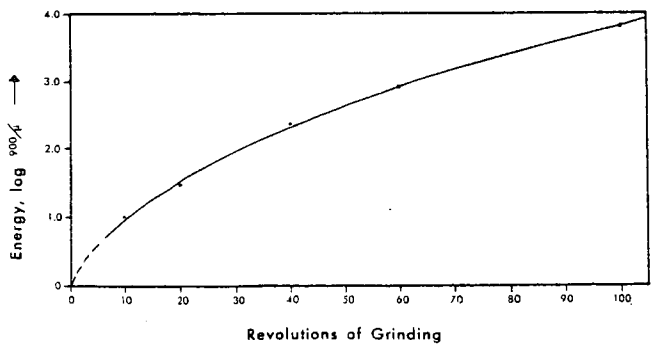

RELATION OF ENERGY FOR GRINDING PREDICTED BY KICK'S LAW TO REVOLUTIONS OF GRINDING (COAL B-19447)

Figure 6

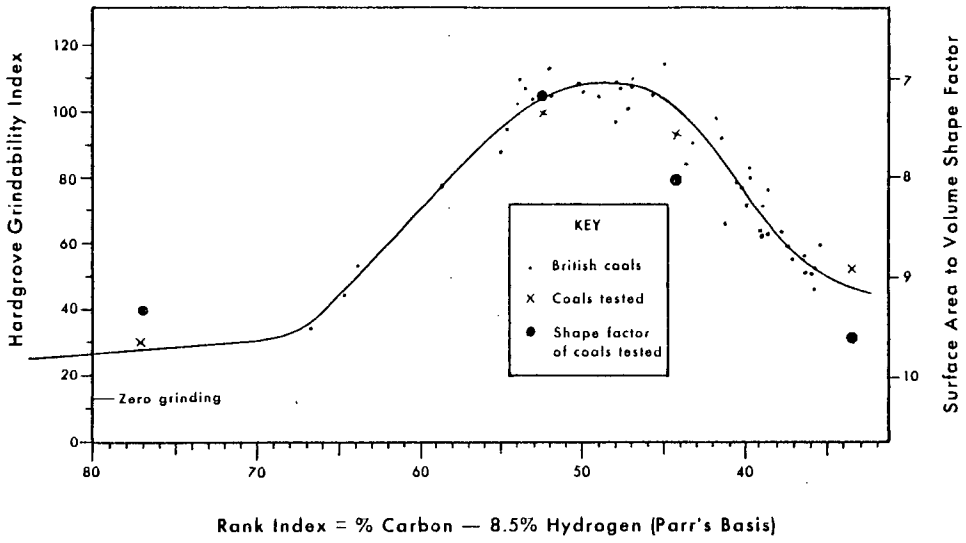

Fig. 7. GRINDABILITY INDEX AND SHAPE FACTOR AS A FUNCTION OF COAL RANK.

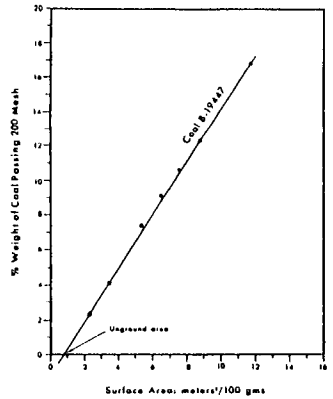

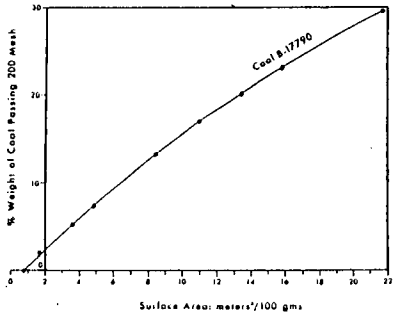

RELATION OF SURFACE AREA TO PERCENT WEIGHT THROUGH 200 MESH
FOR VARYING REVOLUTIONS OF GRINDING IN THE HARDGROVE MACHINE

Figure 8

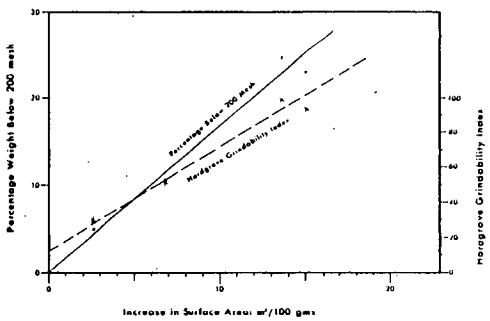

INCREASE IN SURFACE AREA ON GRINDING
ACCORDING TO STANDARD HARDGROVE TEST
AS A FUNCTION OF % WEIGHT THROUGH 200 MESH

Figure 9

Not for Publication
Presented Before the Division of Gas and Fuel Chemistry
American Chemical Society
Atlantic City, New Jersey, Meeting, September 13-18, 1959

Irradiation Studies on Coal and Its By-Products

I. Effect of Radiation and Oxygen at Ambient Temperatures on the Subsequent Plasticity of Bituminous Coals

Frank Rusinko, Jr., Allan Weinstein, and P.L. Walker, Jr.
Fuel Technology Department, The Pennsylvania State University
University Park, Pennsylvania

INTRODUCTION

The effect of radiation on materials is a subject which currently is receiving much attention. Such studies are important because of the changes induced in most materials when they are exposed to radiation. Changes may occur by many mechanisms, such as displacement of atoms caused by energy absorption from incident particles, ionization followed by bond breaking, and formation of free radicals. Studies of the radiation effects in solids indicate that the use of radiation can be a powerful tool for increasing the understanding of the nature of solids.

Organic-type materials, owing to a predominance of convalent bonds or weak van der Waals forces, are more severely changed or degraded than other solids. Changes that may take place in materials are hydrogenation, dehydrogenation, polymerization, cracking, decomposition, and cross-linking, with the degree of change depending upon the type of radiation, incident rate of radiation, extent of radiation time, chemical composition of material, initial state of material, and environment.

Since it is known that gamma radiation can either upgrade or degrade organic materials, a study of the possible effects of gamma radiation on changing the fluidity of bituminous coal is a logical step. For example, a decrease in fluidity for coals high in fluidity would be advantageous, probably resulting in an increase in coke yield and coke strength. On the other hand, an increase in fluidity for coals low in fluidity could result in their becoming satisfactory sources of coke.

EXPERIMENTAL

Coal Samples Used - Eight Pennsylvania bituminous coals were selected for study. Proximate and ultimate analyses of the coals are presented in Tables I and II.

Coal Preparation - The coals were ground to -40 mesh and stored under a nitrogen atmosphere until required for radiation studies. Approximately 50 grams of each coal were placed in quartz or Pyrex containers (4 in. long x 1-1/4 in. inside diameter) and sealed under each of the following conditions:

1. Vacuum - the samples were evacuated until the pressure was less than 10μ Hg and then sealed. The amount of oxygen available to the coal was ca. 2×10^{-6} cc./g.

2. Air - the samples were sealed immediately; these containers held air initially at atmospheric pressure. The amount of oxygen available to the coal was ca. 0.2 cc./g.

3. Oxygen - the samples were evacuated until the pressure was less than 10μ Hg. Oxygen was dosed into the container until the final oxygen pressure was approximately 700 mm. Hg, with the amount of oxygen adsorbed by the coal measured. The containers were then sealed. The amount of oxygen available to the coal was ca. 1.1 cc./g.

Radiation Studies - For radiation studies, the sealed samples were placed in a 40 mil thick cadmium container. Cadmium was used to decrease the slow neutron flux to a relatively low level, since it was desired to irradiate the coals primarily with gamma radiation. The cadmium container with 5 coal samples was lowered down a 3 in. diameter aluminum tube and positioned in the University nuclear reactor. The reactor, which can be classified as a light water cooled, light water moderated heterogeneous type, had its fuel elements located approximately 20 feet under water. Irradiation to a total dosage of 3.8×10^8 rads (requiring about 17 hours) was then carried out at ambient temperatures*. Approximately 90 per cent of the energy absorbed by the coal came from gamma rays and 10 per cent came from fast neutrons.

Gas Analysis - Analysis of the gas in the container following irradiation of the coals was made using gas chromatography. After releasing the gas from the container to the gas analysis system of the chromatographic unit, the gas was dried and its volume measured. The gas analysis was performed using either a 15-ft. #5A molecular sieve column with argon as a carrier gas or a 6-ft. silica gel column using helium as a carrier gas.

Plasticity Measurements - The conventional Gieseler apparatus, modified with auxiliary equipment for better temperature control and more accurate measurement of high fluidity values, was used to determine plastic properties of the coals. The tests essentially were made using the A.S.T.M. Proposed Method of Test (1). However, contrary to recommended procedures, the brake was not applied when the dial divisions exceeded 5 divisions per minute. Instead, the stirrer was allowed to move continuously until it travelled at least 600 dial divisions. For those coals where the stirrer moved more than 600 dial divisions, the brake was then used according to the Proposed Method of Test (1). This procedure was adopted in an attempt to break up the frothy coal mass which formed (and which would go up into the barrel of the Gieseler apparatus and cause sticking) when testing a highly fluid and highly swelling coal.

RESULTS AND DISCUSSION

Analyses of Gases Evolved From the Coals During Irradiation - Table III presents data on the total amount and analysis of the gas evolved from the coals following irradiation in vacuum and oxygen; values for the individual gases are accurate to ±5%. With the present chromatography apparatus, it was not possible to determine water vapor; the gas analyses, therefore, are reported on a dry basis. Other gases, such as ammonia and the oxides of nitrogen

* During the irradiations, it is estimated that the temperature in the coal containers did not exceed 40°C.

which may be formed during the irradiation, were not analyzed for in the present work. Gas analyses have not been reported for the coals irradiated in an air atmosphere because the nitrogen formed following irradiation was a composite of that released from the coal and that added initially in the air. That is, it was not possible to put the results on a basis of gas released from the coal since there was some uncertainty as to the volume of the sample container upon sealing, and hence, uncertainty as to the amount of nitrogen added initially. On the other hand, on the basis of vacuum-irradiation results, no free oxygen was released from the coals. Hence, in the oxygen-irradiation runs (there was oxygen found in the gas following irradiation for three of the coals), the amount of gas released from the coal could be calculated by placing the analyses on an oxygen-free basis.

It is seen from Table III that the amount of gas released from the coals on irradiation at ambient temperatures was quite small in comparison to the total volatile matter content of the coals. More gas was released consistently from the coal upon oxygen irradiation than upon vacuum irradiation, with the ratio of the gas-release volumes ranging from 1.8 to 5.0.

The presence of an oxygen atmosphere during irradiation is seen to have a marked (but not consistent) effect on the analysis of the released gas. As expected, the amount of carbon dioxide and carbon monoxide produced was greatly increased upon oxygen irradiation. The following reactions can be responsible for the increase in the amount of these two gases:

$$O_2 \rightsquigarrow O + O$$
$$C_f + O \rightarrow C(O)$$
$$C(O) \rightarrow CO$$
$$CO + O + M \rightarrow CO_2 + M$$
$$O_2 + O + M \rightarrow O_3 + M$$
$$C_f + O_3 \rightarrow CO + O_2$$

It is noted that a significant amount of carbon dioxide was also released from the coal during vacuum irradiation. It is suggested that this carbon dioxide was a result of decarboxylation of peripheral carboxyl groups on the coal (2,3), release of occluded carbon dioxide from the fine pore system, and/or oxidation of methane (for oxygen irradiation). The second possibility will be considered in more detail shortly.

The effect of radiation and atmosphere on the release of hydrogen from the coals is complex. For coals 167 and 169, release of hydrogen upon vacuum irradiation was negligible. On the other hand, oxygen irradiation of these two coals resulted in a substantial release of hydrogen. For the remainder of the coals, except 166, there was still a somewhat greater amount of hydrogen released upon irradiation in oxygen than in vacuum. For the low volatile coal, 166, the amount of hydrogen released upon either irradiation in vacuum or oxygen was essentially identical.

The effect of radiation and atmosphere on the release of nitrogen from the coals is also complex. For coal 169, the amount of nitrogen released upon oxygen irradiation was appreciably less than that released upon vacuum irradiation. On the other hand, for the other seven coals, oxygen irradiation resulted in the release of considerably more nitrogen than did vacuum irradiation.

From Table III, it is seen that the quantities of methane and ethane produced upon irradiation are very small. Again the results are complex. For methane, oxygen irradiation resulted in increased yields for coals 167, 169, A, and B and decreased yields for the other four coals. For ethane, oxygen irradiation resulted in an increased yield for coal B and a decreased yield for coals 166, 168, 169, C, and D.

Only in the case of coals 166, 167, and 168 was there any residual oxygen present after oxygen irradiation. For these three coals, 37, 11, and 22%, respectively, of the oxygen initially present (approximately 1.2 cc./g. of coal at S.T.P.) was recovered as oxygen following irradiation. This suggests that these coals were especially resistant to oxygen attack (also suggested from plasticity data to be presented later). Considering the large decrease in oxygen pressure during irradiation, the oxygen appearing as carbon dioxide and carbon monoxide in the product gas was small.

At this stage, the effect of the combination of radiation and oxygen atmosphere on the amount of the different gases released from the various coals is not well understood. However, the nitrogen results perhaps permit some understanding. Essentially, the nitrogen could come from three sources - peripheral amino groups, cyclic structures, and occluded nitrogen (4). Radiation, perhaps, would detach peripheral amino groups from the coal structure (the abundance of these groups in coal is small), these groups then reacting with hydrogen atoms to produce ammonia (2). However, in other irradiation studies, as yet unpublished, the authors have found pure ammonia to be quite stable to the radiation used in this research. For example, for a dosage of 10^8 rads, only ca. 0.4 per cent of ammonia (at pressures between 0.1 and 1 atm.) decomposed to hydrogen and nitrogen. Numerous workers (5) have shown that nitrogen present in cyclic groups in coal is largely resistant to removal by oxidation. Therefore, it would appear that the large increase in nitrogen-release from seven of the coals upon oxygen irradiation, in comparison to vacuum irradiation, cannot be explained on the basis of nitrogen-release from cyclic structures.

It seems more reasonable to attribute the majority of the nitrogen coming from the coals to occluded nitrogen. That is, coal is known to be permeated with molecular sized pores (6) which can trap gases. Vacuum irradiation could result in the release of nitrogen from these pores by two mechanisms. First, radiation could produce a small steady-state concentration of nitrogen atoms, which because of their smaller size, could migrate through the molecular openings more rapidly. Second, radiation could increase the magnitude of oscillations of some of the atoms in the coal around the molecular openings, because of their collison with fast neutrons. This increase in magnitude of oscillation would permit a more rapid transport of gas through the molecular openings (7). Oxygen irradiation of coal could result in the release of more nitrogen than that released during vacuum irradiation, since slight oxidation of coal is known to significantly increase the size of the molecular openings (8).

It is of interest to report some results lending support to the suggestion that radiation did enhance the removal of occluded gas from the pores of the coal. Prior to the filling of the quartz containers with oxygen for irradiation studies, the free space of the containers (with coal present) was determined using helium at room temperature for seven of the coals. Following the determination of free space and before filling the containers with oxygen, the coals were outgassed at room temperature to a pressure of

less than 10u Hg for 4 to 6 hours. Despite this outgassing, helium was found in the product gas following irradiation for three of the coals - the amount ranging from a trace for coal 168 to 0.05 cc./g. for coal B. In the case of coal B, the helium constituted ca. 16 per cent of the dry, product gas.

In the light of the conclusions for the source of most of the nitrogen, it is also probable that some of the carbon dioxide (in the vacuum irradiation) and hydrogen released from the coals was originally present as occluded gas.

Whether irradiation in oxygen, rather than in vacuum, is expected to decrease or increase the amount of methane and ethane released is difficult to predict. While enlargement of molecular sized openings during irradiation in oxygen could enhance the release of these hydrocarbons, their radiation-induced oxidation to carbon dioxide and water would decrease their concentration in the released gas. Both effects appear to be operative to varying extents depending upon the coal, as judged from the data in Table III.

Plasticity of Heated Coals Following Irradiation - Gieseler plasticity data were determined on the unirradiated and irradiated coals. At least three plasticity runs were performed on each sample of coal, with the over-all precision being ca. ±15 per cent. The plasticity data are presented in Table IV and Figure 1. Where more than one result is presented for a coal, duplicate irradiations have been performed.

The results clearly show that irradiation in vacuum or in a substantial partial pressure of oxygen can have a marked effect on the subsequent maximum fluidity of heated bituminous coals. Irradiation in the presence of a substantial partial pressure of oxygen generally had more effect on plasticity than did irradiation in vacuum. For six of the coals, vacuum irradiation had a relatively small effect on fluidity. The exceptions were coals A and B, where irradiation reduced maximum fluidities by ca. 50 per cent.

For six of the coals, air irradiation resulted in a significant (and in some cases very large) increase in maximum fluidity. For two of the coals (a low volatile coal and one of the high volatile A coals which showed a significant decrease in fluidity after vacuum irradiation), air irradiation had a negligible effect on fluidity.

The effect of oxygen irradiation on the fluidity of the coals was more varied. For five of the six high volatile A coals, oxygen irradiation substantially lowered the fluidity below that of the corresponding unirradiated coals. For high volatile A coal 168 and the medium volatile coal, oxygen irradiation increased the maximum fluidity over that of the unirradiated coals. Oxygen irradiation had a negligible effect on the fluidity of the low volatile coal.

It is of interest that major changes in fluidity upon irradiation were not accompanied by large changes in the temperatures at which the maximum fluidity occurred. As a typical example, consider coal A. The unirradiated coal had a maximum fluidity of 397 d.d.p.m. at 422°C. The maximum fluidity of the sample irradiated in air was increased markedly to 3566 d.d.p.m., but the temperature of maximum fluidity remained at 422°C.

The effect of pre-oxidation of coal at elevated temperatures and in the absence of radiation on the subsequent coking qualities of coal has

been widely discussed. Many workers (9-14) report that the fluidity of coal, as measured by the Gieseler plastometer, decreases following pre-oxidation. To the authors' knowledge, no published results are available which report that pre-oxidation in the absence of radiation increases the fluidity of coal. However, on the basis of the present results, mild oxidation (that is, with a limited amount of oxygen available to react with coal) promoted by radiation can increase markedly the maximum fluidity of some coals. Whether the same effects can be achieved (and as precisely) by mild oxidation in the absence of radiation will be investigated on the same coals as used in this work.

Work is also being continued in this area directed toward studying the effect of prior irradiation of coal on the nature of the coke and by-products produced upon carbonization. In addition, it is desired to understand the relationships between the chemical and physical properties of coals and the effect of radiation and atmosphere on their subsequent carbonization behavior. As expected, it is not possible on the basis of simple proximate or ultimate analyses to predict these effects.

CONCLUSIONS

The effect of radiation on evolved gas composition and plastic properties of coal is found to vary with the coal being investigated and irradiation atmosphere. Lower rank coals appear to be more affected by the combination of radiation and oxygen atmosphere than do higher rank coals.

By proper selection of atmosphere, together with radiation, the fluidity of coals can be altered to marked extents.

ACKNOWLEDGEMENTS

We would like to express appreciation to G.C. Williams for performing most of the Gieseler determinations. We appreciate the financial support of the Coal Research Board of the Commonwealth of Pennsylvania which made this work possible.

REFERENCES

1. A.S.T.M. Standards on Coal and Coke, Appendix III, p.129, 1954.

2. Breger, C.A., J. Phys. and Colloid Chem., 52, 551 (1948).

3. Tolbert, B.M. and Lemmon, R.M., U.S. Atomic Energy Commission Report UCRL-2704 (1954).

4. Stutzer, Otto and Noe, Adolph C., "Geology of Coal", The Univ. of Chicago Press, Chicago, 1940, p.25.

5. Lowry, H.H., "Chemistry of Coal Utilization", John Wiley & Sons, Inc., New York, 1945, p.478.

6. Anderson, Robert B., Hall, W. Keith, Lecky, James A., and Stein, Karl C., J. Phys. Chem., 60, 1548 (1956).

7. Breck, D.W. and Smith, J.V., Sci. Amer., 200, No. 1, 85 (1959).

8. Walker, P.L. Jr., unpublished results.

9. Rees, O.W., Pierron, E.D. and Bursack, K.F., Illinois State Acad. Sci., 47, 97 (1955).

10. Davis, J.D., Reynolds, D.A., Brewer, R.E. Naugle, B.W. and Wolfson, D.E., U.S. Bur. Mines, Technical Paper No. 702, (1947).

11. Wildenstein, R., Chaleur and ind., 34, 233 (1953). C.A. 47, 12788d, (1953).

12. Lambris, G. and Gerdes, J., Brennstoff-Chem., 22, 125 (1941).

13. Gillings, D.W. and Lawson, W., J. Inst. Fuel, 30, 446 (1957).

14. Inouye, K., Bull. Chem. Soc. Japan, 26, 157 (1953).

TABLE I

PROXIMATE ANALYSES (AIR-DRY BASIS) OF COALS USED

Coal	% Moisture	% V.M.	% C.	% Ash	A.S.T.M. Rank
166	0.9	16.2	73.6	9.3	Low Volatile
167	1.0	26.9	62.1	10.0	Medium Volatile
168	0.6	28.9	61.2	9.3	High Volatile A
169	1.9	38.4	51.9	7.8	High Volatile A
A	2.3	38.1	53.1	6.5	High Volatile A
B	1.8	36.7	55.6	5.9	High Volatile A
C	1.8	36.8	55.2	6.2	High Volatile A
D	1.3	38.2	53.4	5.7	High Volatile A

TABLE II

ULTIMATE ANALYSES OF COALS USED*

Coal	% N	% S	% H	% C	% O	% Ash
166	1.06	1.33	3.80	80.59	5.20	8.02
167	0.92	2.30	4.73	77.86	4.81	9.38
168	0.90	1.73	4.83	78.72	4.50	9.32
169	1.45	1.64	5.07	75.98	7.69	8.17

* Ultimate analyses of Coals A, B, C, and D are not available, as yet.

TABLE III

ANALYSES OF GAS EVOLVED FROM COAL (DRY BASIS) UPON IRRADIATION TO 3.8×10^8 RADS IN VACUUM AND OXYGEN

Coal	Volume of Gas Released cc./g. of coal, S.T.P.	Gas Composition - Per Cent					
		H_2	N_2	CO_2	CO	CH_4	C_2H_6
166-Vacuum	0.048	36.2	7.2	54.8	T	1.5	0.3
166-Oxygen	0.192	8.9	53.2	31.3	6.3	0.3	T
167-V	0.034	0.2	68.9	30.2	T	0.7	0.0
167-O	0.168	26.9	43.5	24.9	4.3	0.5	T
168-V	0.036	50.4	25.7	19.0	T	3.6	1.4
168-O	0.132	26.1	47.0	20.9	5.5	0.6	T
169-V	0.050	0.1	47.0	45.4	1.4	1.0	5.1
169-O	0.148	66.0	3.9	22.3	6.4	1.4	0.2
A-V	0.144	71.4	9.1	16.4	1.8	1.4	T
A-O	0.264	56.5	13.2	24.2	5.0	1.1	T
B-V	0.112	71.4	10.7	14.5	1.3	1.6	0.5
B-O	0.236	53.8	17.2	21.7	5.7	1.2	0.5
C-V	0.064	67.3	11.8	9.0	0.6	10.5	0.8
C-O	0.164	39.3	29.9	22.5	7.6	0.7	0.0
D-V	0.114	76.8	1.9	11.5	1.0	5.6	3.2
D-O	0.314	48.1	29.6	16.3	4.8	0.9	0.3

TABLE IV

EFFECT OF A RADIATION DOSAGE OF 3.8×10^8 RADS AND OXYGEN AT AMBIENT TEMPERATURES ON THE SUBSEQUENT MAXIMUM FLUIDITY OF BITUMINOUS COALS AS DETERMINED BY THE GIESELER APPARATUS

Coal	Initial Softening[1] Temp. °C.	Maximum Fluidity D.D.P.M.[2]	Maximum Fluidity °C.[3]	Solidification Temp.[4] °C.
166	433	1.4	472	494
166-Vacuum	423	1.2	454	488
166-Air	425	1.3	450	472
166-Oxygen	435	0.6	464	499
167	365	451	425	457
167-V	353	610	432	472
167-A	350	822	426	450
167-A	364	935	429	463
167-O	367	1117	440	490
168	347	2767	432	479
168-V	338	2530	427	452
168-V	354	1911	428	481
168-A	339	3936	428	458
168-A	345	3860	428	472
168-O	356	3651	439	489
169	342	1139	424	458
169-V	357	1016	431	468
169-V	337	900	426	460
169-A	337	3193	429	462
169-A	344	3029	427	465
169-O	370	222	436	467
A	348	397	422	457
A-V	347	177	424	458
A-V	350	190	428	458
A-A	344	3566	422	454
A-O	373	124	430	450
B	347	1583	430	462
B-V	351	853	429	461
B-A	349	1484	434	464
B-O	372	701	434	459
C	345	5098	434	470
C-V	347	5207	426	468
C-A	342	6878	423	465
C-O	356	2788	438	475

TABLE IV. (Contd)

Coal	Initial Softening Temp.[1] °C.	Maximum Fluidity D.D.P.M.[2]	Maximum Fluidity °C.[3]	Solidification Temp.[4] °C.
B	345	1778	421	460
D-V	340	1850	422	451
D-A	344	3461	423	456
D-O	356	1083	430	467

1 Temperature of first detectable continuous movement of pointer

2 Dial divisions per minute on the Gieseler scale

3 Temperature of maximum fluidity corresponding to maximum rate of pointer movement

4 Temperature at which pointer shows no further movement

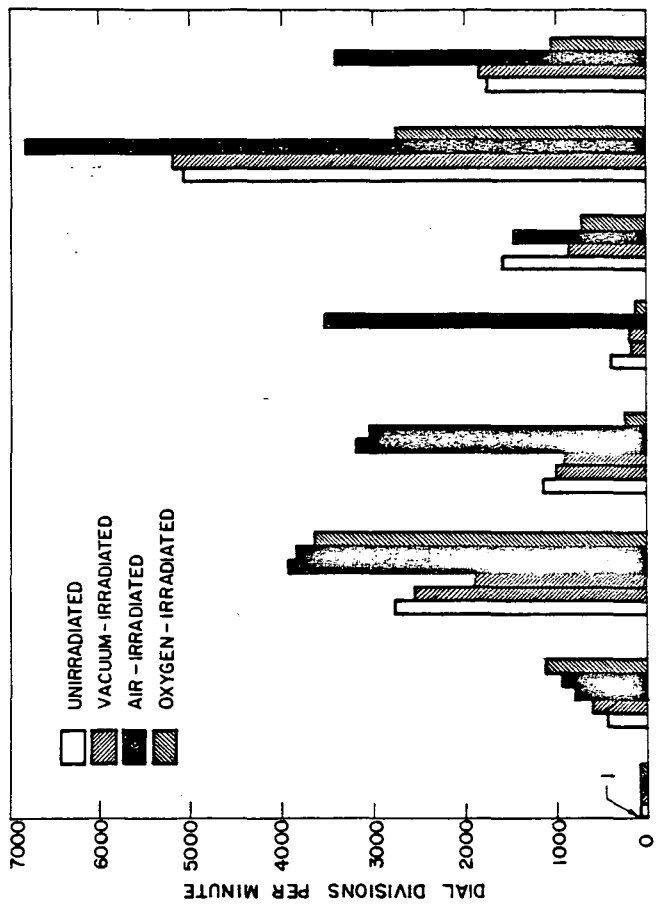

FIGURE 1 - EFFECT OF A RADIATION DOSAGE OF 3.8×10^8 RADS AND OXYGEN AT AMBIENT TEMPERATURES ON THE SUBSEQUENT MAXIMUM FLUIDITY OF BITUMINOUS COALS AS DETERMINED BY THE GIESELER APPARATUS.

Not For Publication

Presented before the Division of Gas and Fuel Chemistry
American Chemical Society
Atlantic City, New Jersey, Meeting, Sept. 13-18, 1959

Effect of Gamma Radiation Upon the Hydrocracking of a Heavy Paraffin

Work done at Columbia University, New York City 27, N.Y.

Present Address of Authors:

Ernest J. Henley, Stevens Institute, Hoboken, New Jersey
Ronald V. Repetti, Wright Patterson Air Force Base,
Dayton, Ohio

Introduction

Although a great deal of work dealing with the effect of ionizing radiation on hydrocarbons at low temperatures has been reported, very little has been published regarding the behavior of these systems at elevated temperatures and pressures. It has been well established that at room temperature pure hydrocarbons ultimately cross link and form insoluble gels (1,2). Recent work has shown that at elevated temperatures the reverse process seems to occur; i.e. degradation of the hydrocarbon molecules (3). If the latter findings are correct, radiation may then be regarded as a potential tool for those industries that customarily employ high temperatures, high pressures, and catalysts, to initiate reactions. An obvious application would be in the gasification processes where coal, waxes, and petroleum stocks are hydrocracked to natural gas substitutes. It was with this potential use in mind that the present investigation was undertaken.

Apparatus -

All runs were conducted in a static system. The reactor, was a type 303 stainless steel pressure vessel rated at 15,000 psia when cold and about 8,000 psia when at working temperatures. A lipless pyrex test tube served as a vessel liner and as a container for the wax samples. The capacity of the reactor with liner was 90 ml., and the entire system (reactor, liner, piping, etc.) had a capacity of 108 ml. Temperature in the autoclave was measured with a copper-constantan thermocouple whose junction was located about one third of the distance up the inside of the reactor. A gage was used whose

nominal pressure reading extended to 5,000 psi. Before using the gage it was calibrated with a dead-weight gage over the range of 200 to 3,000 psia, and was set to read true absolute pressure at 1,500 psia. The maximum deviation over the calibrated range was 20 psia. A blowout disc rated at 4,200 psia was incorporated in the system as a safety precaution. A 750 watt hollow cylindrical heater was employed that afforded a 1/4 in. air bath all around the reactor. Temperature within the reactor was maintained within ± 10°F of the desired level.

The Co^{60} radioisotope used has a half-life of 5.26 years and emits gamma rays of 1.17 and 1.33 m.e.v. per disintegration. The radiation facility is in the form of a pit, 20 in. x 20 in. square and 40 in. deep below ground level, into which a bundle of four 12 in. x 2 in. x 1/8 in. Co^{60} bars can be lowered. In situ dosimetry was accomplished with the Fricke dosimeter. The dose rate was 46,000 R/hr.

Two analytical systems were used, one for gaseous and one for solid products. The small amount of liquid residue produced in some runs was not analyzed. The gaseous products were analyzed with a Perkin-Elmer Model 154 Vapor Fractometer. A combination of packed columns was used that made possible the quantitative analysis of mixtures of hydrogen, nitrogen, argon, and hydrocarbons from C_1 to C_5. A Leeds and Northrup Speedomax Recorder was used in combination with the fractometer. The Perkin-Elmer Company claims for its instrument an analytical reproducibility of ±0.25% and an accuracy of ± 1-2%, both figures being absolute percentages. The actual experimental reproducibility was found to be ± 0.5%.

For those runs where a solid wax residue remained, the wax was examined for evidence of physical change by taking the melting point of the sample. The equipment used was a scaled-down version of the ASTM D87-42 apparatus for the determination of paraffin wax melting points (4). An ASTM 14F paraffin melting point thermometer having a range of 100-180°F and a maximum scale error of 0.2°F was used in the apparatus. In order to check the results obtained by the melting point method, several wax samples were examined for evidence of change by running them, and corresponding control samples, in a standard Beckmann boiling point elevation apparatus. Toluene was chosen as the solvent for these analyses.

Procedure - Experimental

A large quantity of paraffin wax was melted in a 1000 ml. Erlenmeyer flask and while molten, about twenty ml. was poured into each of thirty clean, lipless, pyrex test tubes that had previously been numbered and tared. The samples were then carefully degassed under vacuum. The wax was purchased from the Fisher Scientific Company and had a melting point of 126°F. From a published correlation between melting point and molecular weight (5), it was possible to estimate the molecular weight of this straight chain paraffin to be about 345.

Before charging, the reactor was cleaned thoroughly with a wire brush and then it and all other parts of the system were flushed with acetone. The reactor was then pressure tested, the sample was inserted, and then the system was thoroughly sparged with nitrogen.

To make a run the system was inserted in its heating jacket and the power was turned on. The duration of the initial heating period varied between 30 and 50 minutes, the latter duration being necessary to reach 900°F. The automatic temperature controller then maintained the temperature level to within ± 10°F of the desired setting. At the conclusion of a run the final temperature and pressure were recorded and the reactor was withdrawn from the heater and allowed to cool. About three hours were required for the reactor to cool from 900°F to ambient tem perature.

The gas analysis was complicated by the fact that due to a small amount of liquid present after each run, there existed an equilibrium between the gaseous and the liquid products, hence the composition of the gas is a function of the number of samples taken. Figure 1 shows the variation of product composition with reactor sampling pressure. This difficulty was circumvented in most of the analyses by obtaining, with a syringe, a 50 ml gas sample at a reactor pressure of 500 ± 5 psia and another at 200 ± 5 psia. In this way several analyses of a gas sample could be made in order to determine the reproducibility of the analysis, and it would also be possible to compare the product composition of different runs, provided that they were compared for the same sampling pressure. Toward the end of this investigation a small gas cylinder of 857 ml. capacity became available, and by using it as a reservior into which all of the reactor gas was bled, it

was possible to isolate virtually all of the product gas from the liquid residue in the reactor, and thus arrive at a composition for the total amount of gas produced.

Discussion of Results

Figure 2 shows a plot of reactor temperature vs. pressure as suggested by Shultz and Linden (6). The graph clearly shows that until about 860°F is reached, nothing happens other than heating of the gas in the reactor. At 860°F cracking begins, and because of the additional gas formed, the pressure begins to rise rapidly. The maximum duration of a cracking run was only 5 hours which was not sufficient to attain equilibrium. Figure 2 shows a typical plot of pressure vs. time for a run in progress. Because of the nearly constant rate for run times exceeding 3 hours, no attempt was made to obtain data for very long durations. Instead, runs of 2, 3, 5, and 5 hour duration were made, with the greatest number of duplicate runs at 2 hours. Figure 3 shows typical product spectra for the cracking runs. It is readily seen that the products are almost identical for radiation and for non-radiation runs. This tends to indicate that the same type reaction prevails for both processes, and that if radiation has any influence, it serves merely as an accelerator.

From the experimental data a value of S, designated as the moles of gas formed per gram of wax initially present, was computed for each run. In computing S it was necessary to know n, the number of moles formed during the reaction. Accordingly, a correction factor z was introduced so that at 900°F, the expression $PV = z(nRT)$ would be valid. The factor was computed as the ratio of the actual system pressure at 900°F, (determined by heating a gas with no wax in the reactor) to the perfect gas pressure at 900°F for a comparable quantity of gas. The value of the factor was taken to be 0.78. Figure 4 shows a plot of S vs. run time wherein all the calculated S values for 2 hour radiation runs were averaged to give a point, and the same procedure was followed to obtain the other points shown. The points shown represent the averages of over thirty runs. The initial hydrogen pressure in each run was about 1000 psi.

It is of interest to determine the value of G, which is the number of gas molecules formed per 100 ev. of incident radiation. Figure 5, shows a plot of G vs. run duration. The G values are in the range of 60,000 to 80,000, and are seen to decrease with increasing run duration. The experimental G values are low when compared with the results obtained by Lucchesi, et al. (10) who report a value of about 560,000 for the same conditions. However, the latter value was determined for a short radiation exposure administered during the first minute of cracking. It has been shown in these experiments that the cracking rate is very rapid at first and therefore the G value would necessarily be quite high for shorter duration runs. Figure 5 shows that the G value curve is asymptotic with the ordinate axis and it can be seen that for a run duration of about one minute, the value of G would be appreciably higher than 80,000.

Since the points considered until now have indicated that radiation served to accelerate the cracking reaction, it is important to determine if this conclusion can also be reached by a statistical analysis of the data. The value chosen for comparison between runs was S, the moles of gas formed per gram of wax charged. Since the number of paired sets of radiation and non-radiation runs was small, it was necessary to employ a non-parametric test (7). A suitable one is the Wilcoxon Signed Rank Test (8). By means of it one is able to show that at the 0.025 level of significance radiation has served to increase cracking yields. Or, put in different words, there is a possible error of 2 1/2 percent when one concludes that radiation increases cracking yields.

Acknowledgement

A portion of this work was supported by a grant from the Consolidated Natural Gas Co.

References

(1) Charlesby, A., The Cross Linking and Degradation of Paraffin Chains by High Energy Radiation, Proceedings of the Royal Society (London), vol. 222A, 60 (March 23, 1954).

(2) Lawton, E. J., Balwit, J. S., and Bueche, A. M., The Effect of Initial Molecular Weight on Properties of Irradiated Polyethylene, Industrial and Engineering Chemistry, vol. 46, 1703 (August 1954).

(3) Lucchesi, P. J., Tarmy, B. L., Baeder, D. L., Long, R. B., and Longwell, J. P., High Temperature Radiation Chemistry of Hydrocarbons, Industrial and Engineering Chemistry, vol. 50, No. 6, 879 (1958).

(4) A.S.T.M. D87-42, Standard Method of Test for Melting Point of Paraffin Wax, A.S.T.M. Standards, vol. 5, 14 (1955).

(5) Bennett, H., Commercial Waxes, Chemical Publishing Co., New York, 70 (1956).

(6) Shultz, E. B., and Linden, H. R., Hydrogenolysis of Petroleum Oils, Industrial and Engineering Chemistry, vol. 48, No. 5, 894 (1956).

(7) Hoel, P. G., Introduction to Mathematical Statistics, John Wiley & Sons, Inc., New York, 2nd Ed., 281 (1954).

(8) Bowker, A. H., and Lieberman, G. J., An Introduction to Engineering Statistics, Stanford University, Stanford, California, chapter 7, 32 (September 1957).

FIGURE 1

VARIATION of PRODUCT COMPOSITION
With REACTOR SAMPLING PRESSURE

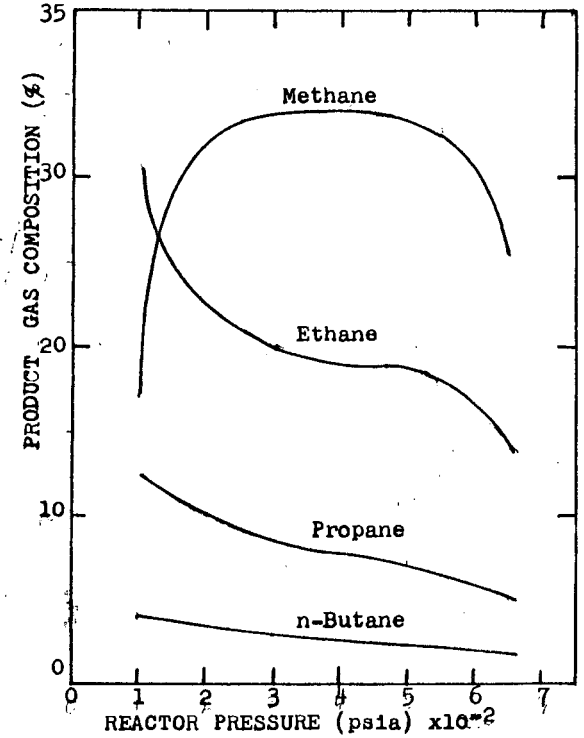

FIGURE II

HEAT-UP CURVE for RUN #56

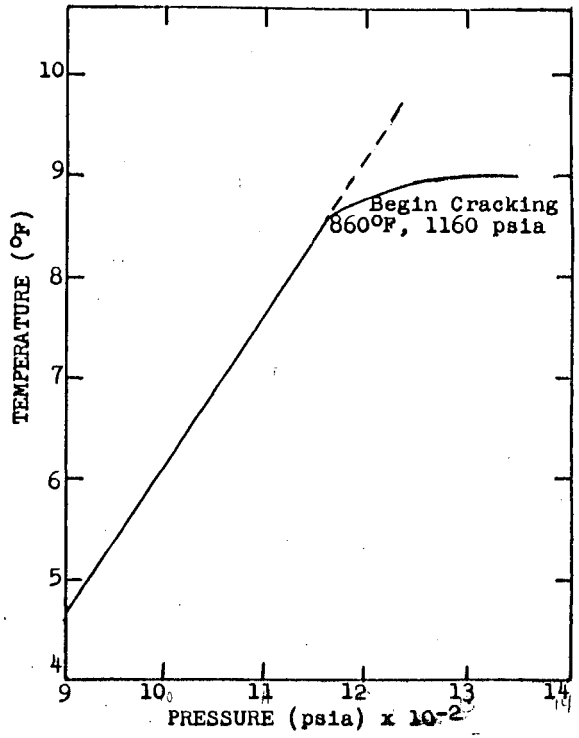

FIGURE III

TYPICAL SPECTRA of PRODUCTS FORMED by HYDROCRACKING

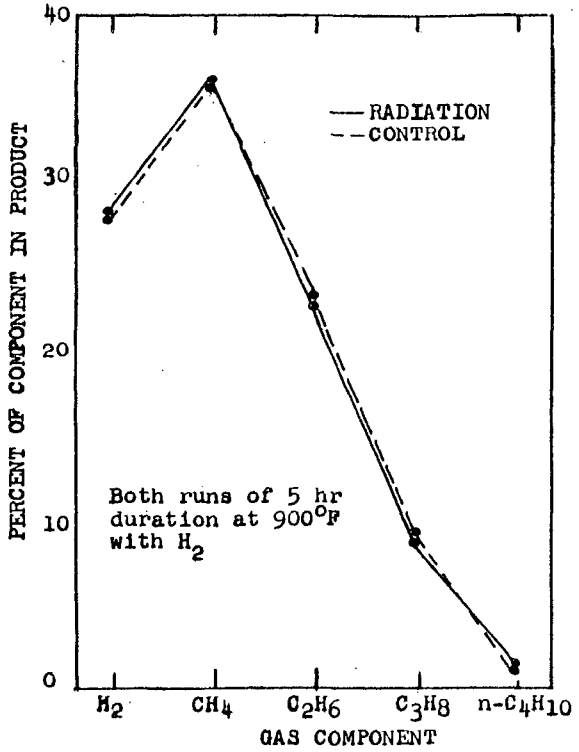

FIGURE IV

VARIATION of S with DURATION of 900°F HYDROCRACKING RUNS

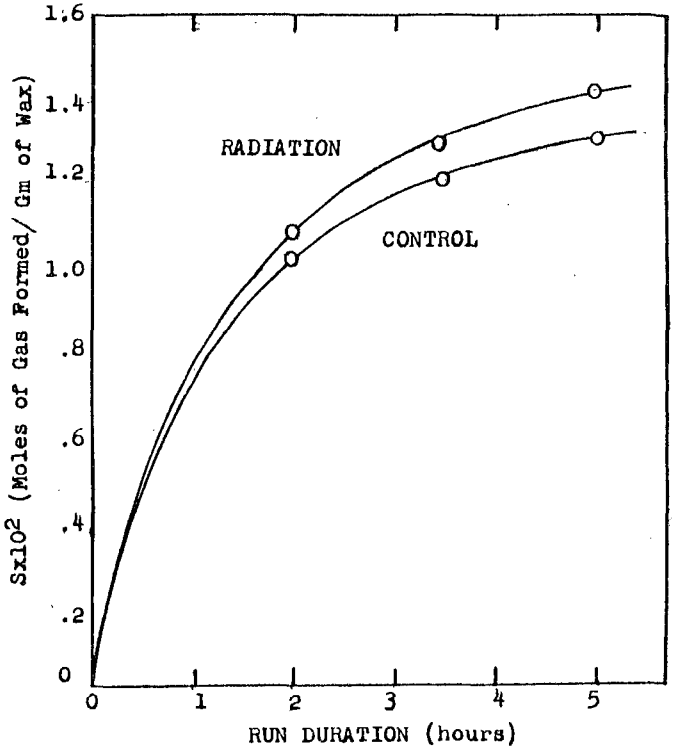

FIGURE V

VARIATION of G withDURATION
of 900°F HYDROCRACKING RUNS